

**Zinc Nanoparticle Enhancement of the Olfactory Neuron Response to Odorants
Associated with Explosives**

by

Christopher H. Moore

A thesis submitted to the Graduate Faculty of
Auburn University
in partial fulfillment of the
requirements for the Degree of
Master of Science

Auburn, Alabama
August 6, 2011

Key words: olfaction, rat, electroolfactogram,
receptors, second messenger, odor tagging

Approved by

Vitaly J. Vodyanoy, Chair, Alumni Professor of Anatomy, Physiology & Pharmacology
Edward E. Morrison, Professor of Anatomy, Physiology & Pharmacology
Eleanor M. Josephson, Associate Professor of Anatomy, Physiology & Pharmacology
John C. Dennis, Research Fellow, Department of Anatomy, Physiology & Pharmacology

Abstract

Many odorants related to manufacturing explosives have low volatilities and have no detectable odor. We found that zinc metal nanoparticles in picomolar concentrations strongly enhanced olfactory receptor neuron responses to odorants related to explosives: Cyclohexanone, Methyl benzoate, Acetophenone, Eugenol. Zinc metal nanoparticles consist of one to two nanometer metallic particles contain 40 to 300 zinc metal atoms, these metal atoms are not in an ionic state. Rat olfactory epithelium was exposed to metal nanoparticles and odorant responses were measured by electroolfactogram (EOG). A small amount of zinc nanoparticles added to explosive odorants strongly increased the odorant response in a dose-dependent manner. In contrast, DMNB (2,3-dimethyl-2,3-dinitrobutane), a volatile organic compound used as a detection taggant for explosives, produced no measurable olfactory response in rat. In physiological experiments enzymatic breakdown of cAMP was prevented by adding the membrane-permeable phosphodiesterase inhibitor IBMX (3-isobutyl-1-methylxanthine). This caused the olfactory cilia cAMP (cyclic adenosine monophosphate) concentration to increase and generated EOG signals. The EOG responses generated by IBMX were not enhanced by zinc nanoparticles. Based on these observations, we hypothesize that zinc nanoparticles are closely located to the interface between the G- protein and the receptor proteins and are involved in transferring signals in the initial events of olfaction. Our results suggest that zinc metal nanoparticles can be used to enhance and

sustain the initial olfactory events and can be used for the dog detection of explosive odorants.

Acknowledgments

The author would like to thank all those who made this work possible through either their direct involvement or through advice and support:

Dr. Vitaly Vodyanoy
Dr. Edward E. Morrison
Dr. John C. Dennis
Mr. Oleg Pustovyy
Dr. Eleanor Josephson
Dr. Elaine Coleman
Dr. Frank F. Bartol

Table of Contents

Abstract.....	ii
Acknowledgments.....	iv
List of Tables	viii
List of Figures	ix
List of Abbreviations	xi
Chapter 1 Introduction	1
Chapter 2.0 Review of Literature	5
2.1 Olfactory Epithelium	5
2.1.1 Supporting Cells	8
2.1.2 Olfactory Receptor Neuron	9
2.1.3 Basal Cells	13
2.1.4 Bowmans Glands	13
2.2. Olfactory Bulb	14
2.4 Signal Transduction pathway in olfaction	15
2.4.1 Odorant Binding Proteins	15
2.4.2 Olfactory Receptor and G_{olf}	16
2.4.3 Other Olfactory G-Proteins.....	20
2.4.4 Antibodies directed against $G_{\alpha i}$ -protein subunits inhibit odorant response	20
2.4.5 RGS2 inhibits olfactory response by attenuating ACIII	21

2.4.6 Odorant specificities and molecular receptive range	21
2.4.7 Combinatorial olfactory receptors & zonal organization.....	21
2.4.8 Adenylate Cyclase & cAMP	23
2.4.9 Cyclic Nucleotide Gated Channels	24
2.4.10 Signal Transduction	24
2.5 Odorants related to explosive	26
2.5.1 Taggant DMNB	30
2.6 Role of zinc in neurobiology and olfaction	31
2.7 Modulation of olfactory response	34
2.7.1 Mechanical stimuli enhances the odorant induced response	34
2.7.2 Zinc nanoparticles enhance olfactory response to odorant	35
2.8 Methods of studying odor-evoked electrical activity	36
2.8.1 Electroolfactogram	39
2.8.2 EOG experiments	40
2.9 Objectives and Specific Aims	41
Chapter 3.0 Materials and Methods	42
3.1 Materials	42
3.1.1 Tools and materials for surgery	42
3.1.2 Non explosive odorants	43
3.1.3 Explosive odorants	43
3.1.4 3-isobutyl-1-methyxanthine (IBMX)	44
3.1.5 Preparation of epithelial slice	44
3.1.6 Zinc nanoparticles	45

3.2 Electroolfactogram.....	47
3.3 Stability of EOG response.....	52
3.4 Delivery of stimuli	52
3.4.1 Odorant delivery	52
3.4.2 Zinc nanoparticle delivery	53
3.4.3 IBMX delivery	54
3.4.4 DMNB delivery	54
3.5 Modulation of EOG responses by zinc nanoparticles	55
3.6 Localization of zinc nanoparticle action	56
3.7 Data development	56
Chapter 4.0 Results	57
4.1 Stability and repeatability of olfactory response	57
4.2 Standard odorant solution with zinc nanoparticles	57
4.3 Explosive odorant solution with zinc nanoparticles	58
4.4 Taggant: DMNB	60
4.5 Comparison of explosive and standard odorants	61
4.6 Location of zinc nanoparticles	62
Chapter 5.0 Discussion	66
Chapter 6.0 Conclusions	71
References	72

List of Tables

Table 1 Physical properties of odorants related to explosives	27
Table 2 Concentration of odorants at LOD levels estimated with K_{aw} values	27
Table 3 Mucus and air LOD levels	28

List of Figures

Figure 1 Location of olfactory epithelium in rat skull.....	7
Figure 2 Functional structure of olfactory system	7
Figure 3 Schematic representation of olfactory epithelial cells.....	8
Figure 4 Schematic representation of olfactory receptor neuron.....	10
Figure 5 Cilia of Olfactory Neuron	11
Figure 6 Sensory transduction	26
Figure 7 A schematic representation of cellular anatomy of the peripheral olfactory system ...	38
Figure 8 EOG setup	48
Figure 9 Experimental setup.....	49
Figure 10 Close-up of EOG measurement system inside a Faraday box	49
Figure 11 EOG measurement system	50
Figure 12 Pressure regulator	50
Figure 13 Profusion chamber and electrode system for IBMX experiments.....	51
Figure 14 Valve control system	51
Figure 15 Odorant applicators for DMNB.....	55
Figure 16 EOG traces recorded from rat olfactory epithelium.....	58
Figure 17 Zinc nanoparticles enhance EOG responses induced by odorants related to the manufacture of explosives	59

Figure 18 EOG traces induced by vapors of explosive odorant solutions with varying concentrations of zinc nanoparticles	60
Figure 19 EOG responses to a taggant, DMNB, and standard odorant solution	61
Figure 20 Comparison of EOG responses induced by the standard and explosive odorants	62
Figure 21 EOG response evoked by IBMX.....	64
Figure 22 Zn nanoparticles do not enhance EOG responses induced by IBMX	65

List of Abbreviations

AC III- Adenylyl Cyclase Type III

AS348- Antiserum for $G_{\alpha s}$

As368- Antiserum for $G_{\alpha q}$

AS6- Antiserum for $G_{\alpha o}$

α subunit- Alpha subunit

β subunit- Beta subunit

γ - subunit- Gamma subunit

K-20- Antiserum for $G_{\alpha o}$

CaBP- Calcium Binding Protein

cAMP- Cyclic Adenosine Monophosphate

cGMP- Cyclic Guanine Monophosphate

CNG- channel- Cyclic Nucleotide Gated Ion Channel

DMNB- 2,3-Dimethyl-2,3-Dinitrobutane

E-17- Antiserum for $G_{\alpha q}$

EOG- Electroolfactogram

EOS- Explosive Odorant Suspension

GABA- Gamma-aminobutyric acid

GDP- Guanosine diphosphate

$G_{\alpha 0}$ - Inhibitory optic neuron G- alpha subunit

$G_{\alpha 0-1}$ - Inhibitory optic neuron G- alpha subunit
 $G_{\alpha 0-2}$ - Inhibitory optic neuron G- alpha subunit
 $G_{\alpha q}$ -G-protein regulate Na^+/K^+ exchange
 $G_{\alpha i}$ - G-protein inhibiting adenylyl cyclase
 $G_{\alpha i-1}$ - G-protein inhibiting adenylyl cyclase, subunit 1
 $G_{\alpha i-2}$ - G-protein inhibiting adenylyl cyclase, subunit 2
 $G_{\alpha i-3}$ - G-protein inhibiting adenylyl cyclase, subunit 3
 G_{olf} - Olfactory G-Protein
 $G_{\alpha s/olf}$ - Stimulatory G alpha-protein
 G_s - G-alpha stimulating adenylyl cyclase
GBC- Glucose Basal Cell
GPCR- G-protein Coupled Receptor
GppNHp- GTP analog guanosine-5'-($\beta\gamma$ -imino)triphosphate
GTP- Guanidine Triphosphate
GTP γ S- Small G protein, Guanosine gamma thio-phosphate
HBC- Horizontal basal Cell
ICAO- International Civil Aviation Organization
IP₃- Inositol Triphosphate
IBMX- 3-isobutyl-1-methylxanthine
LOD- Low odor detection level
NADPH- nicotinamide adenine dinucleotide phosphate
OB- Olfactory Bulb
OBP- Odorant Binding Protein

OE- Olfactory Epithelium

o-MNT- ortho-mononitrotoluene

OR- Odorant Receptor

ORN- Olfactory Receptor Neuron

ORK- Olfactory Receptor Kinase

PBX- Plastic Bonded Explosives

PDE- Phosphodiesterase

PIP₂- Phosphatidylinositol-4,5-bisphosphate

PKA- Protein Kinase A

PETN- Pentaerythritol tetranitrate

RDX- cyclotrimethylenetrinitramine

RGS2- Regulator of G-protein signaling 2

SOS- Standard Odorant Suspension

S1-S6- Transmembrane Domains

⁶⁵Zn- isotope Zinc 65

7TM- 7 Transmembrane Protein

Chapter 1.0 Introduction

Air moves through the nasal cavity in a rostral to caudal direction. In mammals, this air moves over four distinct types of epithelial tissue. The most rostral is the squamous epithelium on the nasal vestibule. Next is a transitional epithelium, consisting of nonciliated cuboidal cells, is located in the main nasal chamber and nasopharynx. The respiratory epithelium, which is pseudostratified columnar ciliated, and is located in the nasopharynx. The most caudal is the olfactory epithelium (Schandar, Laugwitz et al.), located on the caudal portion of the septum that divides the nasal cavity into two halves and on the turbinates in the dorsocaudal aspect of the nasal cavity (Menco and Jackson 1997; Harkema, Carey et al. 2006).

Olfaction is the detection of odorants, volatilized compounds in the air, and pheromones, chemicals that are released from one animal and stimulate a specific behavior or processes (Karlson and Luscher 1959; Phillips and Fuchs 1989; Buck 2005; Brennan and Zufall 2006). The olfactory system has two major divisions: the main olfactory epithelium (Schandar, Laugwitz et al.) and the vomeronasal organ (VNO) (Breer, Fleischer et al. 2006; Ma 2007). The VNO, which is located above the base of the nasal septum, contains the vomeronasal sensory neuron (VSN) that detects pheromones. VSNs have their own type of receptors that project their axons to the accessory olfactory bulb (Firestein 2001; Brennan and Zufall 2006; Munger, Leinders-Zufall et al. 2009; Spehr and Munger 2009). The action of the olfactory epithelium results from physical and

biochemical events that occur in the nasal cavity where olfactory receptor neurons (ORN) interact with odorants. The information received from the sensory neurons is transferred to the secondary neurons in the olfactory bulb (OB). From the bulb, the information is sent to the olfactory cortex where it is used for the discrimination of many odors (Shepherd 1994; Firestein 2001; Buck 2005).

The OE contains olfactory receptor neurons, supporting cells, and basal cells (Getchell, Margolis et al. 1984; Anholt 1989; Phillips and Fuchs 1989; Jones and Rog 1998) . Odorants interacting with the receptors on ORNs must first move into the mucus layer coating the OE. Once in the mucus layer, the odorant interact with odorant binding proteins (OBP). The odorant binding protein is believed to then transport the bound odorant to the olfactory receptor located on the surface of the olfactory cilia (Pevsner and Synder 1990). The rat olfactory genome, like that of most mammals, contains roughly 1500 odorant receptor (OR) genes. However, rats have about 1200 functional OR genes, the rest are nonfunctional pseudogenes (Glusman, Yanai et al. 2001; Gilad, Man et al. 2005; Quignon, Giraud et al. 2005).

Binding of the odorant to the receptor can activate the olfactory specific G-protein, like G_{olf} (Jones and Reed 1989; Firestein 2001). Once activated, G_{olf} activates the olfactory specific adenylyl cyclase, type III adenylyl cyclase (ACIII) which converts ATP to cAMP (Bakalyar and Reed 1990; Firestein 2001). This type of adenylyl cyclase is only present in high amounts in the olfactory cilia (Pace, Hanski et al. 1985). Three of the cAMP molecules produced by adenylyl cyclase bind to the intracellular portion of a

cyclic nucleotide gated (CNG) ion channel and initiate its opening (Firestein 2001). Once the ion channels are open, Ca^{2+} ions enter and the neuron depolarizes by ~ 20 mV (Reed 1992; Firestein 2001). Furthermore, calcium ions, after they enter the cell via these CNG channels, activate calcium gated chloride channels. The chloride ions flow out of the cell and further depolarize the neuron (Kleene and Gesteland 1991; Firestein 2001). When depolarization reaches the axon hillock, at the threshold level, an action potential is generated. The action potential then travels through the unmyelinated axon of the olfactory neuron through the cribriform plate to the olfactory bulb. The olfactory bulb projects to higher brain structures and allows the further processing of the initial odorant induced response.

The exact mechanism through which the olfactory G-protein's and G_{olf} , operate is not fully understood. One hypothesis put forth by Turin (1996) proposed that zinc ion-binding site is positioned near the cytoplasmic end of the sixth transmembrane domain of the olfactory receptor protein. In 2007, it was found that Turin's model was consistent with the physics associated with early olfactory events (Brookes, Hartoutsiou et al. 2007). This model included a proposed electron donor/acceptor functioning as a reducing/oxidizing agent in the intracellular fluid; this agent could be zinc ions.

Metallic nanoparticles were observed in, and isolated from, the blood of humans and other animals (Samoylov, Samoylova et al. 2005). These nanoparticles contain approximately 40-300 atoms bonded with one another to form metallic nuclei. In 2009 zinc nanoparticles were used to enhance the odorant-induced response of the olfactory

neuron by 2.5 fold in a dose dependent and reversible manner (Viswaprakash, Dennis et al. 2009; Vodyanoy 2010). It is the objective of this study to determine whether this nanoparticle enhancement of the odorant induced response applies to odorants used in the manufacture of explosive. Furthermore, this study also aims to determine where in the early events of odorant detection that the nanoparticles exert their modulatory effects. We believe that when odorants associated with the manufacture of explosives are applied to the OE along with zinc nanoparticles, a significant enhancement of the neuronal response can be observed. Our results clearly demonstrate that zinc nanoparticles do cause a significant, dose dependent, enhancement of the response of the olfactory neuron to odorants related to the manufacture of explosives.

Chapter 2.0 Review of Literature

2.1 Olfactory epithelium

In mammals, air flows in through the nostrils in a rostral to caudal direction and moves over the maxilla turbinate, on its way to the olfactory epithelium. The OE is located on the caudal aspect of the septum and on the turbinates. The nasal septum is a cartilaginous structure that separates both halves of the nose (Menco and Morrison 2003; Harkema, Carey et al. 2006). The mammalian nasal cavity contains different numbers of turbinates depending on the species, for example humans have three turbinates (Moran, Rowley et al. 1982; Harkema, Carey et al. 2006) while rats have four (Menco and Jackson 1997; Harkema, Carey et al. 2006). The four rat turbinates are labeled rostrally to caudally I-IV (Menco and Jackson 1997). In mammals, there is a region of transition in the nasal cavity from non-sensory epithelia to olfactory (sensory) epithelia. The inferior, middle, and an aspect of the superior turbinates are covered in the non-sensory epithelium consisting of a columnar epithelium exhibiting cilia or microvilli and goblet cells. The function of this non-sensory epithelium is to warm, clean and humidify inspired air (Morrison and Moran 1995; Menco and Morrison 2003). Both the non-sensory and sensory epithelia possess cilia, but only the sensory epithelium has cilia that function in odorant detection (Morrison and Costanzo 1990). The cilia on the sensory cells increase the surface area available for odorant interaction by 40 times (Menco 1997).

Most vertebrates have similar cellular morphology and organization of the OE (Moran, Rowley et al. 1982; Morrison and Costanzo 1992; Nomura, Takahashi et al. 2004). The olfactory epithelium is pseudostratified ciliated columnar (PSCC) epithelium. Olfactory nerve axons emanating from the receptor neurons, along with mucus secreting Bowman's glands, lymph vessels, and blood vessels, are located below the basal lamina underlying the sensory epithelium (Getchell, Margolis et al. 1984; Anholt 1989; Phillips and Fuchs 1989; Morrison and Costanzo 1990; Jones and Rog 1998; Menco and Morrison 2003). In terrestrial mammals the size of the OE may vary greatly from 4 cm² in humans, to 9 cm² in the rabbit, 20 cm² in the cat (Graziadei 1971), and 50-170 cm² in dogs (Preziuso 1927; Adams 1972; Case 2005).

The olfactory epithelium is coated by a layer of mucus produced by Bowmans glands (Getchell and Getchell 1992). The mucus layer is 20-50 µm thick in primates, and flows at a rate of 10mm/min in man, and the entire mucus sheet is replaced every 10 minutes. Replacing the mucus so quickly facilitates the removal of odorants and airborne contaminants from the olfactory epithelium (Morrison and Costanzo 1990). Several factors affect odorant access to the cilia of olfactory neurons including odorant volatility, odorant solubility in mucus, and the viscosity of the mucus (Pevsner and Synder 1990).

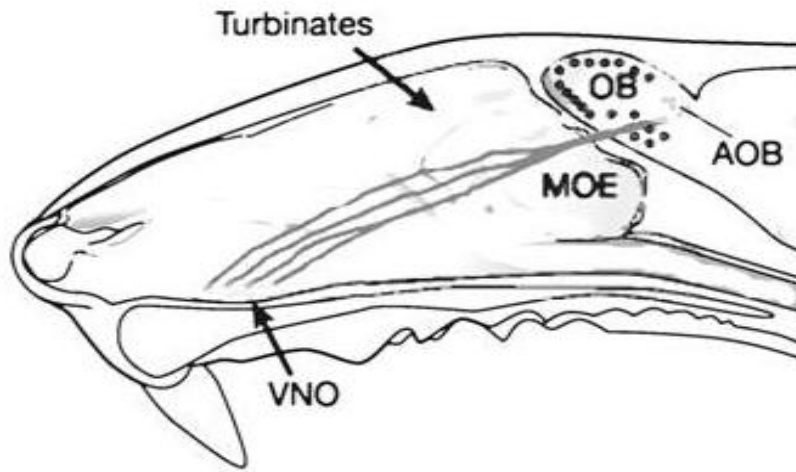


Figure 1. Location of olfactory epithelium in rat skull (redrawn from (Firestein 2001)
 MOE-Main Olfactory Epithelium, VNO- Vomerolnasal Organ, OB- Olfactory Bulb
 AOB- Accessory Olfactory Bulb,

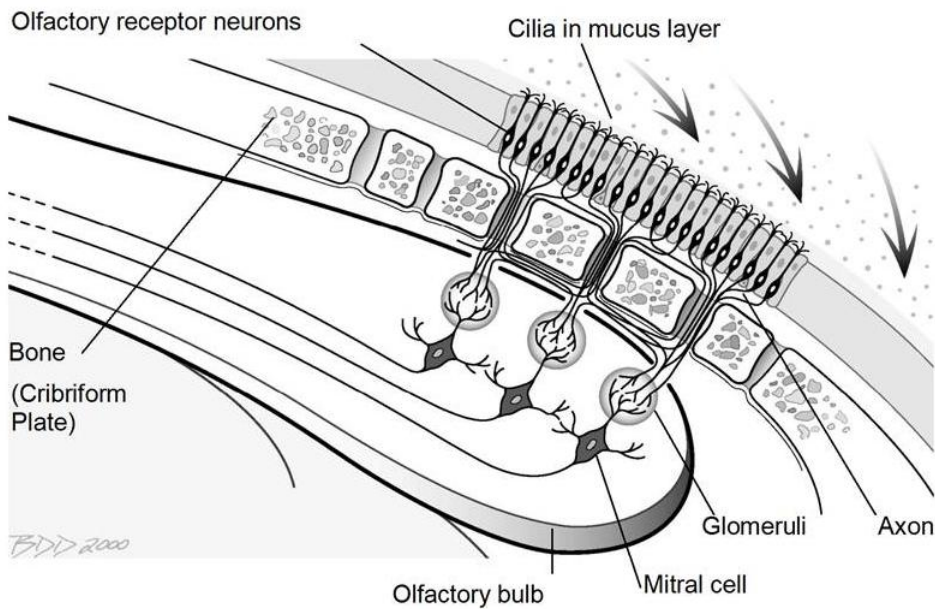


Figure 2. Functional structure of olfactory system (Courtesy of V. Vodyanoy).

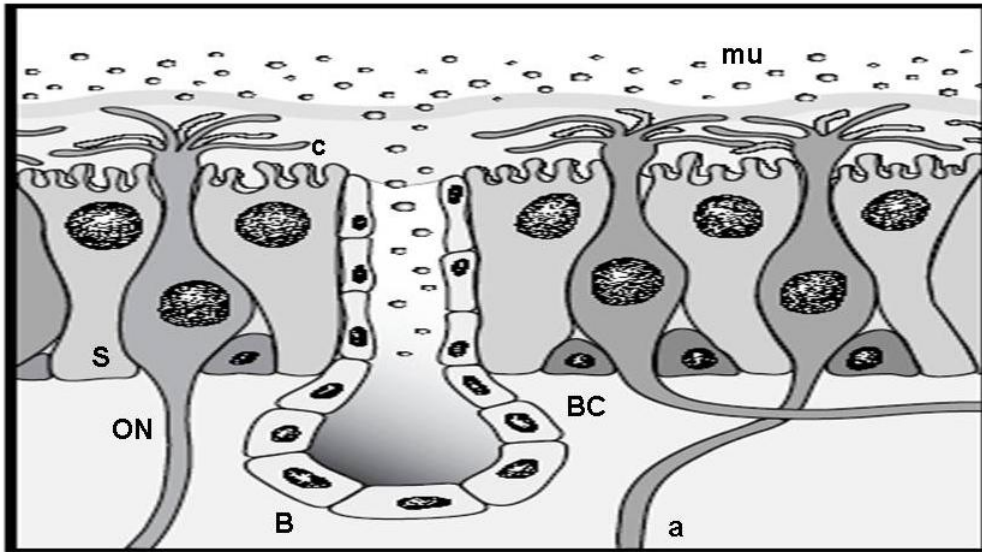


Figure 3. Schematic representation of olfactory epithelial cells (Courtesy of V. Vodyanoy). ON- olfactory sensory neuron, S - supporting cell, BC – basal cell, B – Bowman’s gland, c –cilium of olfactory receptor neuron, a – axon, mu – mucus.

2.1.1 Supporting cells

Supporting cells have an elongated profile with a tapered basal aspect that attaches to the basal lamina (Rafols and Getchell 1983; Menco and Morrison 2003). Microvilli extend from the apical portion of the supporting cells. These cells are closely apposed to both glands and capillaries. The supporting cells insulate the neurons and form tight junctions at their apical surface with the neurons and other neighboring supporting cells (Moran, Rowley et al. 1982; Phillips and Fuchs 1989). Furthermore they can phagocytize degenerating neurons and may act to guide newly formed neurons to their final location (Phillips and Fuchs 1989)

2.1.2 Olfactory receptor neuron

The olfactory receptor neuron (ORN) is the sensory unit of the olfactory epithelium. These are bipolar neurons with a dendritic process ending in cilia in the apical most region and a single axon extending basally from the cell (Figure 3, Figure 4, and Figure 5) (Morrison 1995; Ache and Young 2005). ORN cell bodies are located in the basal two thirds of the neuroepithelium. ORNs produce Olfactory Marker Protein (Frederickson, Giblin et al.). OMP is produced by mature ORNs, those ORNs having developed cilia (Johnson, Eller et al. 1993; Buiakova, Baker et al. 1996; Carr, Walters et al. 1998; Menco and Morrison 2003). OMP is a monomeric globular protein composed of eight β -strands (Wright, Margolis et al. 2005). OMP may play a role in olfactory signal transduction, as mutant ORNs deficient in OMP exhibited a 20-40% reduction in response to odorants (Buiakova, Baker et al. 1996).

While all mature ORNs produce OMP, there are subpopulations of ORNs with that produce other proteins such as odorant receptors, heat shock protein 70, proteins involved in the cyclic GMP cascade, and carbonic anhydrase. Using these criteria there are at least four different subpopulations of ORNs. The first are those that express the odorant receptor in their cilia, these cells will be the focus of this literature review. The other subpopulations include a subset that can be identified by immunoreactivity to heat shock protein 70 (HSP70), which is expressed in their cytoplasm (Carr, Murphy et al. 1994; Menco 1997). Another subset expresses carbonic anhydrase (Brown, Garcia-Segura et al. 1984; Coates 2001), an enzyme that catalyzes the hydration of CO_2 to HCO_3^- and H^+ . These cells are thought to function in the detection of CO_2 (Coates 2001; Hu, Zhong et al.

2007). Yet another subset of ORNs use guanylyl cyclase and cGMP-gated CNG channels rather than ACIII and cAMP-gated CNG channels (Fulle, Vassar et al. 1995; Meyer, Angele et al. 2000).

Vertebrate ORNs are fusiform with a diameter of 4 μm to 14 μm and a length of 22 μm to 28 μm long (Rafols and Getchell 1983; Morrison and Costanzo 1990), although some have been measured to be 42 μm long (Moran, Rowley et al. 1982). The soma is primarily occupied by the nucleus (Rafols and Getchell 1983). Adjacent to the nucleus, along the periphery of the cell the rough endoplasmic reticulum and Golgi body can be observed (Moran, Rowley et al. 1982).

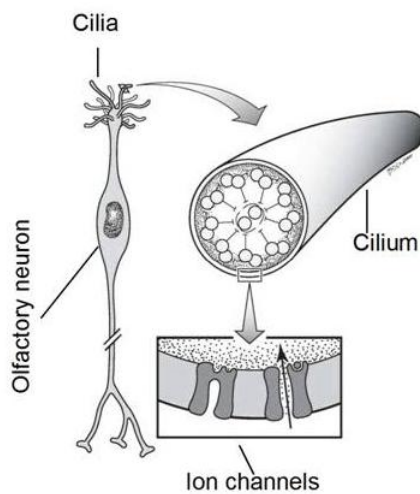


Figure 4. Schematic representation of olfactory receptor neuron. (Courtesy of V. Vodyanoy)

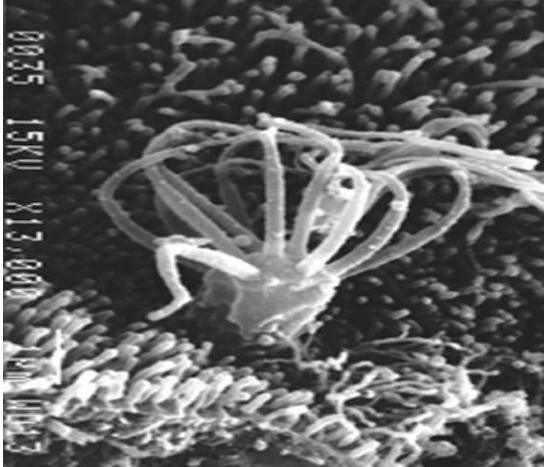


Figure 5. Cilia of Olfactory Neuron (center) can be seen emanating from the dendritic bulb of the ORN (Courtesy of E. Morrison). Surrounding the ORN are the supporting cells (Courtesy of Dr. E. Morrison). The cilia of the ORN are the sites of olfactory transduction, and therefore contain all the necessary components: olfactory receptors, G_{olf} , adenylyl cyclase, and cyclic nucleotide gated ion channels.

The ORN dendrite originates from the soma of the cell and extends apically and terminates in the dendritic knob above the cell (Moran, Rowley et al. 1982; Rafols and Getchell 1983; Morrison and Costanzo 1990). The dendritic knob has an elongated spherical shape and is 0.5 μm to 2 μm in diameter, with rats having a diameter of 0.5 μm (Moran, Rowley et al. 1982; Costanzo and Morrison 1989; Morrison and Costanzo 1990; Nomura, Takahashi et al. 2004). In rats, the density of dendritic knobs varies from as high as 60,000 knobs/ mm^2 in some areas to 10,000 knobs/ mm^2 in others (Menco and Jackson 1997). From each knob, 20-30 sensory cilia project above the surrounding cells, into the mucus layer (Figures 5) (Moran, Rowley et al. 1982; Menco 1997; Firestein 2001; Menco and Morrison 2003; Nomura, Takahashi et al. 2004). The ORN cilia can range in length from as short as 1 μm to over 30 μm (Morrison and Costanzo 1990). The cilia have a 9+2 pattern of organization similar to that of motile cilia (Figure 4).

Although their structure is similar to that of motile cilia, the ORN cilia lack the dynein arms necessary for motility (Moran, Rowley et al. 1982; Satir and Christensen 2007).

ORN cilia have long been thought to be the site of olfactory transduction (Gesteland, Lettvin et al. 1965; Getchell 1986; Kurahashi 1989). OR specific antibodies have been found to bind to the proximal and distal portions of the cilia, therefore indicating that the cilia are indeed the site of olfactory transduction (Adamek, Gesteland et al. 1984; Menco, Bruch et al. 1992; Menco 1997). On its surface, each cilium expresses odorant receptor proteins, and contains adenylyl cyclase (AC) type III, G_{olf} and cyclic nucleotide gated ion channels (Zufall, Firestein et al. 1991; Menco, Bruch et al. 1992; Menco 1997; Firestein 2001; Menco and Morrison 2003).

From the basal of the ORN, a single unmyelinated axon extends through the basal lamina. The axons themselves are 0.1-0.4 μm in diameter. The axons form small intraepithelial bundles before traveling through the basal lamina (Costanzo and Morrison 1989; Morrison and Costanzo 1990; Morrison 1995). Bundling of these axons puts them in close proximity to one another and allows them to interact. This interaction occurs as a result of ions being exchanged between axons. As one axon is conducting an action potential, it may depolarize a neighboring axon and thereby increase the amplitude of the signal reaching the olfactory bulb (Eng and Kocsis 1987).

As these bundles continue toward the cribiform plate they form larger axon fascicles, which are 20-40 μm in diameter and are surrounded by ensheathing cells. The fascicles

pass through the cribriform plate of the ethmoid bone (Morrison and Costanzo 1990; Doucette 1993; Morrison 1995). The axons in the fascicles then synapse in glomeruli of the olfactory bulb (Morrison and Costanzo 1990; Menco and Morrison 2003).

2.1.3 Basal Cells

Basal cells are located near the basal lamina, below the ORN and supporting cells (Figure 3). There are two types of basal cells, horizontal (HBC) and globose (GBC) (Graziadei and Graziadei 1979; Holbrook, Szumowski et al. 1995; Menco and Morrison 2003).

HBC's and GBC's are roughly 4-7um in diameter and have a round, centrally located nucleus. They are rounded or cuboidal and have rough cellular surfaces (Morrison and Costanzo 1990). The globose basal cells undergo mitosis normally and following insult to the existing neurons and develop into fully functional olfactory neurons (Harding, Graziadei et al. 1977; Caggiano, Kauer et al. 1994). As the globose basal cells differentiate into neuron, they do so in zones. Each growth zone is composed of columns of receptor cells surrounding a supporting cell with basal cells below. The turnover of old neurons occurs over a period of 4-8 weeks (Costanzo 1985; Phillips and Fuchs 1989)

2.1.4 Bowman's glands

Bowman's glands are acinar glands and are composed of pyramidal cells with a spherical nucleus and short stubby microvilli. These cells surround a central lumen (Figure 3) (Menco and Morrison 2003; Nomura, Takahashi et al. 2004). In most mammals Bowman's glands have both serous and mucus secretions (Seifert 1971; Getchell and Getchell 1992). In general, Bowmans glands in mammals are composed of two different kinds of cells, one cell type is found within the basal region of the olfactory epithelium

and produces a mucus secretion. The second type is located near the base of the lamina propria and produces a serous like secretion (Getchell and Getchell 1992). Myoepithelial cells are located around the secretory cells of the glands. The myoepithelial cells squeeze the secretory cells and move the secretory products toward a simple duct, which extends through to the epithelial surface (Breipohl 1972; Menco and Morrison 2003). The mucus secreted by the Bowmans glands contains odorant binding proteins that transport odorants through the mucus layer (Getchell and Getchell 1990; Pevsner and Synder 1990).

2.2 Olfactory Bulb

The axons from the ORNs terminate in the olfactory bulb. The olfactory bulb is organized into seven layers: the olfactory nerve layer, the glomerular layer, the external plexiform layer, the mitral cell layers, the internal plexiform layer, and the granule cell layer. Each glomerulus is a specialized collection of neuronal processes of several mitral cells and interneurons that receive axons from multiple ORN's. Depending on species, approximately 15,000-25,000 ORN axons terminate in a single glomerulus. Therefore the glomeruli are designed for effecting spatial summation of impulses from the OE (Allison and Warwick 1949; Allison 1953; Shepherd, Getchell et al. 1975; Greer 1991; Kimmelman 1993). The axons also synapse on the inhibitory periglomerular interneurons as well, which in turn synapse on adjacent glomeruli. The ORN axons enter each glomerulus and divide repeatedly before making excitatory synapses onto the dendrites of the mitral cells. The mitral cells, located deep to the glomeruli and the tufted cells, generate part of the output information from the olfactory bulb to higher brain

centers. Tufted cells also generate olfactory bulb output. The granule cells, which are deep to the mitral/tufted cells, synapse on secondary dendrites of the mitral cells through which they exert an inhibitory effect and the mitral and tufted cells and extend collaterals to the basal dendrite of the granule cells. The granule cells receive excitatory input from central brain regions: locus coeruleus, olfactory nuclei, and the piriform cortex. The axons from the mitral/tufted cells form olfactory tracts which divide into medial and lateral striae. The tracts project to the piriform cortex, anterior olfactory nucleus, amygdala, and entorhinal cortex. From these structures connections are made with the hippocampus, hypothalamus, and thalamus (Allison and Warwick 1949; Allison 1953; Kimmelman 1993). In the olfactory bulb, odor generated action potentials can have both excitatory and inhibitory effects (Ottoson 1971).

2.4 Signal transduction pathway in olfaction

Olfactory receptor neurons convert odorant molecule binding events into an electrical response that eventually generates an action potential that transmits this response to brain. The initial events in the signal transduction pathway include a series of biochemical steps that occur in the cilia of the olfactory neuron. These events are schematically shown in Figure 6.

2.4.1 Odorant binding proteins

Odorant binding proteins (OBPs) are low molecular-weight soluble proteins in the nasal mucus of vertebrates and in the sensillar lymph of insects (Pevsner and Synder 1990; Pelosi 1994). OBPs are members of a family of proteins known as lipocalins. Lipocalins are ligand binding proteins with a common structure of eight parallel β -strands that fold

to form a β -barrel, at the center of which is a ligand binding site (Boudjelal, Sivaprasadarao et al. 1996). They have been shown to reversibly bind odorants and have relatively low specificity for ligands (Pevsner and Synder 1990).

2.4.2 Odorant receptor and G_{olf}

There are two classes of ORs, the fish like Class I ORs (Ngai, Dowling et al. 1993) that detect water soluble odorants, and the mammalian Class II ORs that detect volatile odorants (Freitag, Ludwig et al. 1998). In 1991, Buck and Axel reported the discovery of a large multigene family of seven transmembrane (7TM) proteins that are expressed in the OE. Buck and Axel suggest that these OE specific 7TM proteins may be odorant receptors (OR) (Buck and Axel 1991). ORs constitute the largest gene family in vertebrate animals (Glusman, Yanai et al. 2001; Zhang and Firestein 2002; Quignon, Kirkness et al. 2003). Humans possess 1000 OR genes with 300 of these genes being functional; the rest are nonfunctional pseudogenes (Glusman, Yanai et al. 2001; Gilad, Man et al. 2005). Chimpanzees have a total of about a 1000 total OR genes with 350 being functional (Gilad, Man et al. 2005). Other animals such as canines and mice have nearly 1300 OR genes and around 1000 genes that are functional (Zhang and Firestein 2002; Quignon, Kirkness et al. 2003; Olender, Fuchs et al. 2004). Rats have roughly 1500 OR genes, of which about 1200 are functional (Quignon, Giraud et al. 2005).

ORs are members of the seven transmembrane (7TM) G-protein coupled receptor (GPCRs) family, meaning that ORs interact with a GTP-binding protein (G-protein) and that the receptor has seven membrane spanning segments (Buck and Axel 1991; Kobilka

1992; Lancet, Benarie et al. 1994; Breer 2003; Menco and Morrison 2003; Gaillard, Rouquier et al. 2004; Fredholm, Hokfelt et al. 2007). ORs are similar to adrenergic receptors (Odowd, Hnatowich et al. 1989), which can serve as a functional model for GPCRs such as ORs (Kobilka 1992). Like other members of the 7TM GPCR family, ORs consist of three extracellular loops that alternate with three intracellular loops to join the seven transmembrane segments. ORs also have an N-linked glycosylation site within the N-terminal extracellular segment. There are conserved cysteine residues within the first and second extracellular loops. These cysteine residues are believed to form a disulfide bond. There is also a conserved cysteine within the C-terminal intracellular domain that serves as a palmitoylation site securing the domain to the membrane (Buck and Axel 1991). Mutation of these C-terminal cysteines to glycine, in adrenergic receptors, results in a nonpalmitoylated form of the receptor that cannot stimulate adenylyl cyclase possibly due to an inability to couple to the G-protein (Odowd, Hnatowich et al. 1989). Transmembrane regions 3 through 5 show the greatest amount of sequence divergence. These regions are thought to be involved in ligand binding (Kobilka, Kobilka et al. 1988; Buck and Axel 1991; Kobilka 1992). This diversity provided by the sequence divergence would enable the olfactory receptor (OR) to bind a multitude of odorants (Buck and Axel 1991; Mombaerts 1999).

ORs and other 7TM GPCRs use G-proteins to generate intracellular signals. Portions of the fifth and sixth hydrophobic domains may be involved in coupling the receptor to the G-protein (Kobilka, Kobilka et al. 1988). When complexed with the G-protein, the receptor has a higher affinity for its ligand (odorant). A heterotrimeric G-protein, like the

olfactory G-protein (G_{olf}), has three subunits: G_α , G_β , and G_γ . When the receptor binds the odorant, the G_α subunit dissociates from the receptor and the $\beta\gamma$ dimer. The α subunit loses its affinity for GDP and binds GTP because there is a higher concentration of GTP than GDP in the cell. The free G_α subunit can now activate adenylyl cyclase until the GTP bound on the G_α is hydrolyzed to GDP by the intrinsic GTPase activity of the α subunit. At which point the G_α subunit re-associates with the $\beta\gamma$ dimer on the GPCR (Kobilka 1992; Sandhya and Vemuri 1997).

There are many models attempting to explain OR recognition of odorants, we will discuss two of them; the stereochemical model and Turin's inelastic electron tunneling model. The stereochemical model was put forth by Moncrieff in 1949 (Moncrieff 1949) and advanced by Amoore in 1963. The stereochemical model states that the molecular shape of the odorant is recognized by the OR (Amoore 1963). In this model there are seven primary odor categories into which all odorants can be placed. The seven primary odors are ethereal, camphoraceous, musky, floral, minty, pungent, and putrid. These odors are said to be primary because they have "rigid" primary valences. Therefore these primary odor molecules are said to be unlikely to fit into more than one kind of receptor site. Amoore reviewed several studies that lend support to the stereochemical model. Saunders demonstrated that odors in the same primary odor category fit the same receptor site using ether, camphor, musk, floral, and minty (Saunders 1962). Johnston demonstrated that complex odors can be synthesized using multiple primary odors by using camphoraceous, musky, floral, and minty odors to reproduce the cedar-wood odor (Johnston 1963). Johnston and Sandoval used three representative musk samples

(aromatic nitric musk, the macrocyclic musks, and tetralin musk), compounds thought to be so chemically distinct, that they could not stimulate the same receptor. When these odorants were presented to trained odor judges, the judges were unable to differentiate between the three odors. This would suggest that at least musk is valid primary odor category (Johnston and Sandoval 1962; Amoore 1964). Unfortunately, the stereochemical model cannot explain the difference in odor of the deuterated compounds that have the same shape (Turin 1996; Haffenden, Yaylayan et al. 2001; Franco, Turin et al. 2011).

The second model was suggested by Turin in 1996. Turin suggested that each odorant has a specific vibrational frequency that the OR recognizes. Turin proposed that a zinc ion-binding site is positioned near the cytoplasmic end of the sixth transmembrane domain of the olfactory receptor protein. When the odorant is bound to the receptor, an electron donor like NADPH donates an electron. The electron is transferred through the receptor to the zinc ion which then breaks the disulfide bond between G_{olf} and the OR. Once the disulfide bond is broken G_{olf} is then free to activate ACIII (Turin 1996). In 2007, it was found that Turin's model was consistent with the physics associated with early olfactory events (Brookes, Hartoutsiou et al. 2007). This model included a proposed electron donor/acceptor functioning as a reducing/oxidizing agent in the intracellular fluid; this agent could be zinc ions.

Jones and Reed (Jones and Reed 1989) reported the discovery of an olfactory specific G-protein that they termed G_{olf} . They analyzed immunoblots of protein extracts derived from the olfactory turbinates of normal or bulbectomized animals. Removal of the

olfactory bulb (bulbectomy) is known to degenerate the ORN. The levels of an olfactory specific protein, olfactory marker protein (Frederickson, GIBLIN et al.), are known to decrease as a result of the ORN degeneration (Graziadei, Margolis et al. 1977; Graziadei and Graziadei 1979). After the bulbectomy was performed, G_{olf} was found to be absent from the OE, while G_{olf} was found in the OE of non-bulbectomized rats. The loss of G_{olf} from the OE corresponded with the loss of OMP from the OE (Jones and Reed 1989) meaning that G_{olf} like OMP was a olfactory specific protein. A G_{olf} specific antiserum was used to analyze immunoblots of partially purified olfactory sensory cilia, where G_{olf} was found in high concentration. Further immunocytochemical analysis showed that G_{olf} was localized in the dendritic knobs and cilia thereby implicating these structures as the location of odorant detection and olfactory transduction (Jones and Reed 1989) (Figure 6).

2.4.3 Other olfactory G-proteins

There are other types of G-proteins present in the olfactory epithelium beside G_{olf} . Using AS348, an antibody that recognizes the c-terminus region of G_s and G_{olf} , revealed that these proteins were located in the olfactory cilia rather than the rest of the olfactory epithelium. Western blotting using C10, an antibody that recognizes the C-terminal decapeptide of G_{ai-1} , G_{ai-2} , and G_{ai-3} , demonstrated the presence of these three inhibitory G-proteins in the cilia, OE, and cerebral cortex with similar concentrations in each sample tissue. From this, the investigators deduced that G_i subtypes are not enriched in the cilia. The antibodies AS368 and E-17 were used to observe the presence of G_{aq} subtypes. G_{ao-1} and G_{ao-2} were found in the olfactory cilia through the use of the antibodies AS6 and K-20 (Schandar, Laugwitz et al. 1998).

2.4.4 Antibodies directed against $G_{\alpha i}$ -protein subunits inhibit odorant responses by reduction of cAMP level in olfactory cilia.

The odorant-induced accumulation of cAMP can be inhibited by antibodies directed against $G_{\alpha s/olf}$. In contrast, antibodies raised against $G_{\alpha i}$ -subunits caused a strong enhancement of the odorant-induced cAMP accumulation. Western blotting and immunoelectron microscopy revealed the presence of both $G_{\alpha s/olf}$ - and $G_{\alpha i}$ -subunits in rat cilia preparations. The existence of both stimulatory and inhibitory odorant-induced regulation of adenylyl cyclase activity in olfactory cilia may indicate that an initial integration of different odorant stimuli begins at the level of primary reactions in the same effector enzyme (Sinnarajah, Ezeh et al. 1998). These results were confirmed by whole cell patch-clamp experiments with olfactory sensory neurons (unpublished results).

2.4.5 RGS2 inhibits olfactory responses by attenuating adenylyl cyclase III activation

The regulator of G protein signaling (RGS2) reduces cAMP production by odorant-stimulated olfactory epithelium membranes, where the $G_{\alpha s}$ family member $G_{\alpha olf\alpha}$ links odorant receptors to adenylyl cyclase activation. RGS2 reduces odorant elicited cAMP production independent of an effect on $G_{\alpha olf\alpha}$, but by acting as an inhibitor of adenylyl cyclase type III, the predominant adenylyl cyclase isoform in olfactory neurons. Whole cell voltage clamp recordings of odorant stimulated olfactory neurons indicate that endogenous RGS2 negatively regulates odorant-evoked intracellular signaling. These results reveal an effective mechanism for controlling the activities of adenylyl cyclase, which likely contributes to the exquisite ability of olfactory neurons to discriminate odors (Sinnarajah, Dessauer et al. 2001).

2.4.6 Odorant specificities and molecular receptive range

The sensitivity of ORNs depends on the odor receptor proteins they express on the cilia surface. It has been demonstrated by pharmacological methods that ORNs manifest high specificities to certain molecules (Araneda, Kini et al. 2000). This ORN property allows the olfactory system to be both highly selective, and able to recognize many odorants.

2.4.7 Combinatorial olfactory receptors and zonal organization of the Olfactory Epithelium

The olfactory neurons in mammals express only one of the multitude of olfactory receptors (Vassar, Ngai et al. 1993; Malnic, Hirono et al. 1999). An odorant is recognized by a combination of olfactory receptors that is unique for that odorant. Furthermore, a single odorant receptor may recognize multiple odorants. Therefore, an odorant may be recognized by overlapping but non-identical combinations of olfactory receptors, the combinatorial system of odorant recognition allows for the identification of the large number of odorants. Furthermore, odorants at different concentrations are recognized by different combinations or codes of receptors. This would indicate that an odorant may have a different odor at different concentrations (Malnic, Hirono et al. 1999; Buck 2004).

The olfactory epithelium has been suggested to be organized by olfactory receptor specificity. Therefore based on the receptor subfamily expressed, the olfactory epithelium can be divided into three or four regions (Ressler, Sullivan et al. 1993; Strotmann, Wanner et al. 1994; Strotmann, Wanner et al. 1994). Within an expression

zone an odorant receptor gene can be expressed at random in the neuronal population. The high degree of homology within OR subfamilies, coupled with the presence of multiple OR subfamily members in a single expression zone indicates that the receptors in each zone may recognize the same odorant or a closely related group of odorants (Ressler, Sullivan et al. 1993).

Thus the initial organization of the olfactory response information may occur via related receptors, located next to one another, detecting related odorants (Ressler, Sullivan et al. 1993). These regions exhibit bilateral symmetry in the two nasal cavities (Ressler, Sullivan et al. 1993). Therefore, each subfamily of receptor is expressed in several bands that extend along the anterior-posterior axis of the nasal cavity as well as the medial-lateral axis. What is more is that nearly identical arrangement of the olfactory epithelium are seen in different individuals regardless of gender (Ressler, Sullivan et al. 1993).

2.4.8 Adenylyl cyclase and cAMP

The presence of adenylyl cyclase III (ACIII) in olfactory cilia and its role in olfactory transduction was revealed by Pace et al in 1985 (Pace, Hanski et al. 1985) (Figure 6). Like other members of the adenylyl cyclase family, type III adenylyl cyclase converts ATP to cAMP (Bakalyar and Reed 1990; Firestein 2001). The activation of single odorant receptor leading to the activation of AC III can induce the production of 2×10^5 molecules of cAMP/s/cell (Takeuchi and Kurahashi 2005). The function of this enzyme is enhanced by GTP, Forskolin, guanosin 5'(β,γ -imido) triphosphate (GppNHp) and guanosin 5'-0-(3-thio) triphosphate (GTP γ S) (Pace, Hanski et al. 1985). Furthermore, the effects of adenylyl cyclase can be enhanced by using phosphodiesterase inhibitors,

thereby preventing the degradation of the cAMP, thus allowing it to continue to exert its effect (Pace, Hanski et al. 1985).

ACs in general function as coincidence detectors, and thus integrate signals while reducing the signal to noise ratio. They may integrate IP₃ signals with those of cAMP, via Ca⁺² activated calmodulin activated by Ca⁺² influx stimulated by IP₃. The calmodulin then may enhance the performance of AC. This would serve to reduce background noise as it requires both pathways to be activated, thus preventing activation by another means, such as incidental Ca⁺² influx (Anholt 1994).

2.4.9 Cyclic nucleotide gated channels

The cyclic nucleotide gated channels (CNG channels) consist of six transmembrane domains S1-S6. S4 is homologous to the voltage sensor of voltage gated channels. The channel also has a domain that is homologous with the cyclic nucleotide binding site of cAMP and cGMP dependent protein kinases (Bonigk, Altenhofen et al. 1993; Firestein 1994). It requires three molecules of cAMP binding to the cAMP binding site to activate the olfactory CNG channels. These channels are not voltage dependent and exhibit voltage dependent block by extracellular divalent cations, thereby providing a means of adaptation since Ca⁺² is known to permeate the cyclic nucleotide channels (Frings, Lynch et al. 1992; Zufall, Hatt et al. 1993). The channels are open for approximately 1.5 ms and close within 0.2 ms – 1 ms depending on if just a single channel is open or if several channels are open (Firestein and Werblin 1989; Firestein, Shepherd et al. 1990).

2.4.10 Signal transduction

Once in the mucus layer, the odorant interacts with odorant binding proteins (OBP). OBPs exhibit an affinity toward odors and pheromones, bind odorants and pheromones specifically, reversibly, and saturably. This would suggest that OBP plays a role in olfactory perception (Pevsner and Snyder 1990; Pelosi 1994). Binding of the odorant to the seven transmembrane odorant receptor can lead to the activation of an olfactory specific heterotrimeric G-protein, G_{olf} (Jones and Reed 1989; Firestein 2001) (Figure 6). Once activated G_{olf} exchanges GDP for GTP, dissociates from the $\beta\gamma$ subunit, and activates a type III adenylyl cyclase which converts ATP to cAMP (Bakalyar and Reed 1990; Firestein 2001).

Each G_{olf} molecule may activate one AC III which in turn can produce approximately 1000 cAMP molecules per second. Three molecules of cAMP must bind to the intracellular portion of a cyclic nucleotide gated (CNG) ion channel in order to initiate its opening. Once the channels is open, the Ca^{2+} enters the cell and the ORN membrane potential drops from -65mV to about -45mV, thus depolarizing the cell and initiating the action potential that travels down the axon to the olfactory bulb (Firestein 2001). Once the signal has been terminated, G_{α} reunites with the $\beta\gamma$ subunit and awaits another activating signal from an odorant.

Although the cAMP pathway appears to be the dominant olfactory transduction pathway in mammals (Brunet, Gold et al. 1996) the cAMP pathway is not the only pathway through which information about odorants is conveyed. Certain odorants, such as lylal

and isovaleric, activate the G-protein $G\alpha_o$, which once activated dissociate into $\beta\gamma$ and α subunits. The α -subunit stimulates phospholipase C instead of AC III to degrade PIP_2 into the second messengers IP_3 and DAG. IP_3 binds and activates IP_3 gated calcium channels. This allows Ca^{+2} to influx into the cell. The calcium binds to calcium- gated Na/K channels. Calcium also binds to K channels to facilitate the repolarization of the cell (Restrepo 1996).

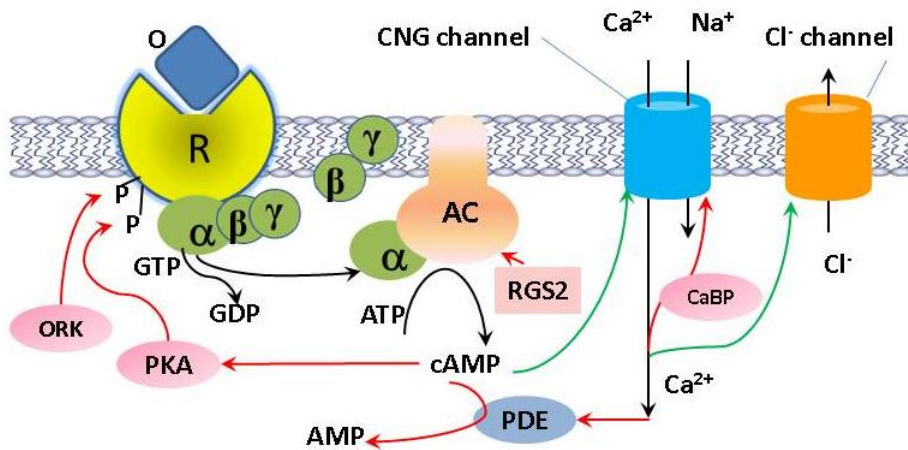


Figure 6. Sensory transduction. AC, adenylyl cyclase; CNG channel, cyclic nucleotide-gated channel; PDE, phosphodiesterase; PKA, protein kinase A; ORK, olfactory receptor kinase; RGS2, regulator of G proteins; CaBP, calmodulin-binding protein. Green arrows indicate stimulatory pathways; red indicates inhibitory (feedback).

2.5 Odorants related to explosives

Explosives produce a variety of odors composed of the the odor(s) emanating from the explosive material itself, as well as additional odors related to land mine manufacture, packing, and casting. Those explosives based on TNT and other aromatic nitrates are known as cast explosives. Polymer bonded explosives (plastic explosives) involve the nitramine or nitrate ester explosives; they include RDX and PETN (Harper, Almirall et

al. 2005). Explosives that are buried underground produce additional odors resulting from interaction with ground and water (Jenkins, Leggett et al. 2001).

The list of odorants associated with explosives beyond the parent components includes 2,4-dinortoluene, 2-ethyl-1-hexanol, phthalates, diphenylamine, ethyl centralite, 2,4-dinitrobenzene, 1,3-dinitrobenzene, 2-ethyl-1-hexanol and methyl centralite (Harper, Almirall et al. 2005). In the research program “RealNose”, DARPA (Defense Advanced Research Projects Agency) identified an additional list of compounds related to explosives (Kruse 2007). Physical properties, low detection levels, and concentration in olfactory mucus for several odorants related to manufacturing of explosives (Kruse 2007; SWGDOG 2007) are given in Tables 1-3.

Table 1. Physical properties of odorants related to explosives

Odorant	^a Vapor pressure, mm Hg	^b Solubility in water, g/l	Molecular weight, g/mol
Cyclohexanone	4.33	25	98.14
Methyl benzoate	0.38	2.1	136.15
2,4 DNT	0.00165	0.27	182.14
Amyl Acetate	3.5	1.7	130.19
+/-Limonene	1.88	0.0138	136.23
Heptanal	3.52	0.126	114.19
Acetophenone	0.397	6.13	120.16
Eugenol	0.0226	2.47	164.2
Ethyl vanillin	8.84E-4	2.82	166.17
2-Heptanone	3.86	4.3	114.19

a, b, data (at 25 °C) from <http://www.syrres.com/esc/physdemo.htm>

Table 2. Concentration of odorants at LOD levels estimated with K_{aw} values

Odorant	Odor	LOD Ppb	Concentration in air, M/l	$^cK_{aw}$	Concentration in mucus, M/l
Cyclohexanone	Acetone	^a 10	4.45×10^{-10}	9.14×10^{-4}	4.87×10^{-7}
Methyl benzoate	Fragrant	^a 10	4.45×10^{-10}	1.33×10^{-3}	3.36×10^{-7}
2,4 DNT	Almond	^a 0.5	2.22×10^{-11}	5.98×10^{-5}	3.72×10^{-7}
Amyl Acetate	Banana	^a 0.002	8.9×10^{-14}	1.44×10^{-2}	6.17×10^{-12}
+/-Limonene	Turpentine	^a 10^3	4.45×10^{-7}	0.99	4.46×10^{-7}
Heptanal	Dairy	^b 1.2	5.3×10^{-11}	0.17	3.11×10^{-10}
Acetophenone	Orange	^c 1.0	4.45×10^{-11}	4.18×10^{-4}	1.06×10^{-7}
Eugenol	Spicy	^d 0.2	8.9×10^{-12}	8.08×10^{-5}	1.10×10^{-7}
Ethyl vanillin	Vanilla	^c 0.1	4.45×10^{-12}	2.80×10^{-6}	1.59×10^{-6}
2-Heptanone	Fruity	^c 10	4.45×10^{-10}	5.51×10^{-3}	8.07×10^{-8}

^aCanine levels of detection given by Agency. ^bLOD in mice(Laska, Joshi et al. 2006).

^cLOD estimated by a model (Hau, Connell et al. 2000; Abraham, Gola et al. 2002).

^dCanine LOD (Myers 2008). ^eAir/water partition coefficient. LOD – low odor detection level for dogs.

Table 3. Mucus and air LOD levels

Odorant	Mucus, M	Air, M
Cyclohexanone	4.9×10^{-7}	4.45×10^{-10}
Methyl benzoate	3.4×10^{-7}	4.45×10^{-10}
2,4 DNT	3.7×10^{-7}	2.22×10^{-11}
Amyl Acetate	6.0×10^{-10}	8.9×10^{-14}
+/-Limonene	4.5×10^{-7}	4.45×10^{-7}
Heptanal	3.1×10^{-10}	5.3×10^{-11}
Acetophenone	1.1×10^{-7}	4.45×10^{-11}
Eugenol	1.1×10^{-7}	8.9×10^{-12}
Ethyl vanillin	1.6×10^{-6}	4.45×10^{-12}
2-Heptanone	8.1×10^{-8}	4.45×10^{-10}

The odorant concentration delivered to the OE receptors was not known and needed to be estimated. The odorant concentration in the bottle headspace was estimated from the water/air partition coefficient K_{aw} . K_{aw} was calculated from the vapor pressure value, solubility in water and molecular weight (Tables 1-2) by the following equation derived from Henry's law (Amoore and Buttery 1978): $K_{aw} = ((55.5/S - 0.0555) \times M + 1) \times P \times 0.97 \times 10^{-6}$. P is the vapor pressure in mm Hg, S is solubility in water

in g/l of the pure odorant at 25 °C, and M is its molecular weight. The concentrations of odorants in mucus for canine detection levels are shown in Table 2. Concentrations of eight odorants are in a range of 0.1-0.5 μM, one is ~0.3 nM, and the lowest one is ~ 6 pM.

In intact olfactory mucosa, the partition coefficient between odorant in air and mucus is enhanced by odorant binding proteins (OBP). OBPs are secreted in the nasal mucus of terrestrial vertebrates, and usher odorants to their neuronal receptors (Pevsner, Sklar et al. 1986; Nespoulous, Briand et al. 2004). The true partition coefficient for amyl acetate can be calculated from experimental data of interaction of amyl acetate and OBP (Pevsner, Sklar et al. 1986).

The partition coefficient estimated from binding data for amyl acetate to purified OBP is equal to 1.5×10^{-4} . Using this coefficient the concentration of amyl acetate in the mucus is estimated to be 6.0×10^{-10} M. This is 2 orders of magnitude higher than that found from the air/water partition coefficient. Similarly, the partition coefficient estimated from experimental data on interaction of methyl benzoate with lysine (main moiety of OBP) is equal to $\sim 6 \times 10^{-4}$. Therefore the concentration of this odorant in mucus at the LOD concentration is $\sim 7.4 \times 10^{-7}$ M (Zhou, Illies et al. 1993).

As a result of our final estimate, the concentrations of target odorants in olfactory mucus at the LOD levels are shown in Table 3. The concentrations of target odorants in mucus at the canine LOD levels shown on Table 3 are not as low as the canine LOD concentrations in air.

One may suspect that among such a large number of chemical compounds related to explosives, there are some chemicals that may be neurologically toxic or detrimental to olfaction. Detector dogs represent the fastest, most versatile, reliable real-time explosive detection device available. Instrumental methods, while they continue to improve, generally suffer from a lack of efficient sampling systems, selectivity problems in the presence of interfering odorant, and limited mobility (Furton and Myers 2001). Moreover, in order to avoid injury in experiments with canines and minimize potential harm by explosive odorants, initial experiments that defined neurotoxicity and olfactory damage were carried out with rodent and other animal models (Corcelli, Lobasso et al. 2010).

The recent work by Corcelli and colleagues exemplifies the analysis of odors associated with explosives. They identified some volatile organic compounds released from the different plastic and/or rubber components of landmine cases and carried out EOG and Ca^{2+} imaging experiments on rat olfactory mucosa. After studying six chemical compounds associated with explosives and explosive devices they have been able to activate olfactory receptors (Corcelli, Lobasso et al. 2010).

2.5.1 Taggant: DMNB (2, 3-dimethyl-2, 3-dinitrobutane)

A taggant is a compound added to materials to allow detection of that material. In our work we were concerned with taggants added to explosives. Taggants are volatile chemicals that evaporate slowly from the explosive to enable the detection of the explosive material. In 1991 the International Civil Aviation Organization (ICAO)

convention on the Marking of Plastic Explosives for the Purpose of Detection directed that detection agents be incorporated into plastic bonded explosives (PBX) (ICAO 1991). ICAO chose four compounds as taggants for PBX material: Ethylene glycol dinitrate (EGDN), 2,3-dimethyl-2,3-dinitrobutane (DMNB), ortho-mononitrotoluene (*o*-MNT), and para-mononitrotoluene (*p*-MNT) (ICAO 1991; BCST 1998). In the United States, the primary taggant is DMNB (Connolly, Curby et al. 1998). DMNB is incorporated into PBX at 0.5% by mass (ICAO 1991) and is reported to be easily detected by canines and special devices in concentrations as small as 0.5 parts per billion in air (BCST 1998; Steinfeld and Wormhoudt 1998; Yinon 2003; Yinon 2005; Yinon 2006; Wynn, Palmacci et al. 2010). However studies have indicated that DMNB may not be detectable by trained detector canines (Furton and Myers 2001; Harper, Almirall et al. 2005). Nonetheless, there has been no effort to determine this electrophysiologically.

2.6 Role of zinc in neurobiology and olfaction

Zinc in various forms, ionic or metallic, has been shown to play different and sometimes conflicting roles in biology and olfaction. It has been well documented that zinc plays an important role in neurobiology (Frederickson and Bush 2001; Frederickson, Koh et al. 2005; Frederickson, Giblin et al. 2006). In humans, low serum zinc levels can lead to anorexia, dysfunction of smell or anosmia, and taste, as well as cerebellar and mental dysfunction. Henkin (Henkin, Patten et al. 1975) demonstrated that zinc loss was indeed the cause of many neurological dysfunctions. In the human brain, zinc appears to modulate the overall excitability of the brain via glutamate and GABA receptors (Frederickson, Koh et al. 2005). Takeda et al observed via the injection of ⁶⁵Zn into the

olfactory bulb, the accumulation of Zn in ipsilateral piriform cortex, amygdaloidal nuclei, the anterior commissure, and the ipsilateral entorhinal cortex. Following another injection of amygdala nuclei, ⁶⁵Zn was observed twenty four hours later in the ipsilateral piriform and entorhinal cortex. This would suggest the intraneuronal transport of zinc along the olfactory tract (Takeda, Ohnuma et al. 1997) .

However, this may not be the only role that zinc ion plays in olfaction. Mackay-Sim and Dreosti (Mackay-Sim and Dreosti 1989) observed that mice on zinc deficient diets fail to show food odor preference, the ability to distinguish between a preferred food and food that the animal usually avoids. Subsequent histological studies revealed that no damage had been done to the olfactory epithelium. Thus, the zinc deficiency presumably had a negative effect on the enzymatic components of smell (Mackay-Sim and Dreosti 1989). Furthermore, it has been demonstrated that zinc ions can cause anosmia in humans as it has been documented that individuals using intranasal sprays containing zinc have reported anosmia. The zinc ion in the compound was found to be the only possible suspect as other components of the spray were known to have no effect in olfaction (Alexander and Davidson 2006). Additionally it has been documented that zinc sulfate can cause anosmia or hyposmia in mice in as little as one hour (McBride, Slotnick et al. 2003).

Zinc ions can modulate olfactory bulb and olfactory epithelial (Schandar, Laugwitz et al.) neuron excitability (Horning and Trombley 2001; Aedo, Delgado et al. 2007). This modulation in neuron excitability has been observed experimentally by invoking ion

channel-zinc ion interactions. Micromolar zinc ionic concentrations modulated neuronal activity via a zinc ion-sodium channel interaction in OE neurons (Aedo, Delgado et al. 2007). Such interaction is consistent with observed inhibition of the voltage-gated sodium current caused by 1 mM zinc ions in dissociated rat olfactory receptor neurons (Seebungkert and Lynch 2002). Zinc ions at a concentration of 25 μ M were shown to modulate electro-olfactogram (EOG) of the frog (Ishimaru 2000). By using Forskolin, an AC stimulator, and IBMX, a phosphodiesterase inhibitor, to generate EOG responses, a significant and reversible attenuation of signals was observed. The authors explained that attenuation as zinc ion blockage of cyclic nucleotide ion channels by zinc ion.

Furthermore, copper and zinc ions can inhibit the function of G_{α} (Gao, Du et al. 2005). G_{α} governs the production of cAMP during excitation and consequently these ions inhibit olfactory signals. It was earlier demonstrated that zinc ion inhibition of adenylyl cyclase correlated with conformational changes in the enzyme (Klein, Sunahara et al. 2002; Klein, Heyduk et al. 2004).

Some zinc containing compounds are incorporated into powerful explosives (Gur'ev, Gordopolov et al. 2006). A known detonator, zinc-sulfide, decomposes and produces zinc and sulfur compounds, which are very detrimental for the olfaction process (Slotnick, Glover et al. 2000; McBride, Slotnick et al. 2003; Slotnick 2006; Slotnick, Sanguino et al. 2007).

In 1996, Luca Turin proposed that Zn ions transduce the signal from the OR to the G-protein via inelastic electron tunneling. In inelastic tunneling, the OR would receive electrons from a donor such as NADPH. These electrons pass to G_{olf} when an odorant is in the receptor's binding site, at which time the electrons from the donor reduce the disulphide bridge between the G-protein and receptor enabling the G-protein to elicit its effects in the enzymatic cascade (Turin 1996).

All the above effects produced by zinc are related to the **zinc ions**. In contrast, a strong enhancement of olfactory responses by very small concentrations of **zinc metal nanoparticles** has been reported (Viswaprakash, Dennis et al. 2009). The metal zinc nanoparticle is composed of a relatively large number of neutral atoms. For example, 1-nm zinc nanoparticles contain ~ 40 atoms, a 2-nm particle has ~300 atoms. The physical, chemical, and catalytic properties of metal nanoparticles are different from those of ions and bulk metals (Thomas 1988; Aiken and Finke 1999; Viswaprakash, Dennis et al. 2009; Viswaprakash, Josephson et al. 2010; Vodyanoy 2010).

2.7 Modulation of olfactory response

The response of the OE has been observed to be modulated by methods other than direct contact with odorants.

2.7.1 Mechanical stimuli enhance the odorant induced response

Olfactory neurons are able to respond to mechanical stimuli resulting from air flow (Ueki and Domino 1961; Grosmaître, Santarelli et al. 2007) . Using a whole cell patch clamp

system (Grosmaître, Santarelli et al. 2007) examined the effects of mechanical stimuli, air pressure ejections without odorant, on responses of mice olfactory receptor neurons. The response curve of the mechanical stimuli resembled that of the odorant induced response, suggesting the mechanical response is mediated by a second messenger cascade. Using adenylyl cyclase inhibitors, a cocktail of 10 mM forskolin (an adenylyl cyclase activator) and 100 mM 3-isobutyl-1-methylxanthine (IBMX, a phosphodiesterase inhibitor), or knocking out the cyclic nucleotide-gated channel CNGA2, the authors were able to block the mechanical stimuli induced response, thereby indicating that the mechanical stimuli were transduced using the cAMP pathway. They further demonstrated that mechanical stimuli enhanced the odorant induced response. The enhancement by mechanical stimuli was dose dependent and the single neuron current excited by 1 μ M octanoic acid, increased by three fold when air pressure increased from 20 to 40 p.s.i. Additionally, they showed that this mechanosensitivity enhances the firing frequency of individual neurons when they were weakly stimulated by odorants (Grosmaître, Santarelli et al. 2007).

2.7.2 Zinc nanoparticles enhance olfactory response to odorant

Viswaprakash and colleagues demonstrated that a very small concentration of zinc metal nanoparticles in a range of a few fM to 450 pM can strongly enhance electroolfactogram (EOG) or whole cell patch-clamp responses to odorant (Viswaprakash, Dennis et al. 2009; Vodyanoy 2010). Adding a small amount of these particles to an odorant can increase the responses to the odorant by a factor \sim 2.5. Zinc nanoparticles produce no odor effects alone, but only enhance the action of applied odor if applied in mixture. At these concentrations, effects are dose-dependent and reversible. The particles are

spontaneously cleared from the system, providing a specific, sensitive, and effective means of regulation of initial olfactory responses.

It was shown that extracellular or intracellular perfusion of these particles can increase the responses to the odorant by a factor ~ 7 . Copper, gold, and silver nanoparticles were found to not produce any effects similar to those found for Zn. When zinc nanoparticles are replaced by Zn^{+2} -ions at the same concentrations range they observed a reduction of the odorant response by olfactory receptor neurons.

Viswaprakash and collaborators, hypothesized that zinc nanoparticles are closely located to the interface between G- protein and receptors and involved in transferring signals in initial events of olfaction. There is a significant difference between zinc ions and zinc nanoparticles as ions are single charged atoms and nanoparticles are clusters of uncharged atoms (Viswaprakash, Dennis et al. 2009).

2.8 Methods of studying odor-evoked electrical activity

There are several methods for electrophysiological recording of olfactory events. These methods are based on measurement of odor-evoked electrical activity recorded at the different levels of signal of transduction. The methods for electrophysiologically studying the OE include the patch clamp and electroolfactogram are illustrated in Figure 7 (Blanton, Lo Turco et al. 1989).

The patch clamp technique allows one to measure ion currents in cells. Erwin Neher and Bert Sakmann developed the patch clamp and received the Nobel Prize in Physiology and Medicine in 1991 for their work (Hamill, Marty et al. 1981). In a patch clamp, a pipette is pressed against a single cell (Figure 7, inset a) thereby forming an electrical seal with that cell; these seals can be made in the range of 10-100 G Ω . This high level of resistance can reduce the amount of background noise in electrophysiological recordings (Hamill, Marty et al. 1981).

The electrical activity of the OE has been studied since the 1930's (Scott and Scott-Johnson 2002). But it was Ottoson in 1956 who coined the term electroolfactogram (Ottoson 1956). In an electroolfactogram (EOG) a saline filled electrode with relatively large opening (5-50 μm) is used to study summated receptor potentials of many olfactory receptor neurons (Ottoson 1971; Scott and Scott-Johnson 2002) (Figure 7, inset b).

There are other methods used to study olfaction at various levels. By piercing the epithelial surface with a metal-filled microelectrode one can measure odorant-induced extracellular spike activity in single neurons (Gesteland, Lettvin et al. 1965) (Figure 7, insets c and d). By using bipolar wire electrodes, spike activity from a bundle of olfactory axons can be recorded (Getchell 1973) (Figure 7, insets e and f). Similarly to olfactory epithelial neurons, olfactory bulb neurons can be studied with saline pipettes and microelectrodes (Ottoson 1960; Nakashima, Mori et al. 1978) (Figure 7, insets g and h).

There is evidence of a direct correlation between electroolfactogram amplitude and intensity of human odor perception (Doty, Kreiss et al. 1990). Due to the existence of

multiple explosive odorants which require multiple ORs for detection, we will use the electroolfactogram. Our long term objective is to enhance the dogs perception of explosive odorants. The EOG method will enable us to study the summated odor-evoked electrical activity of several olfactory receptor neurons at once.

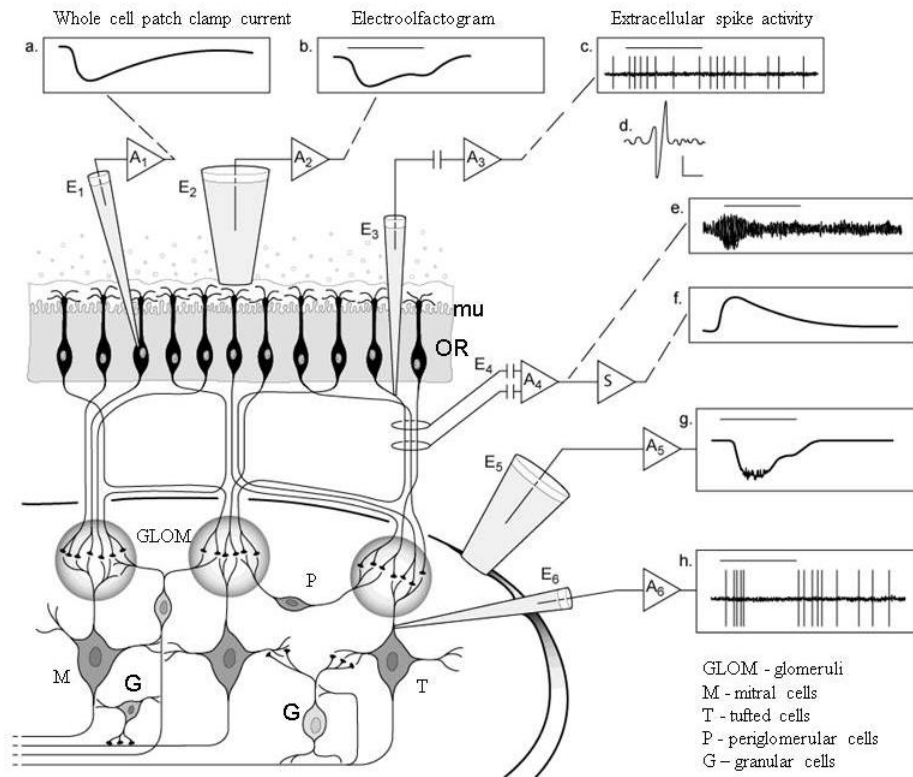


Figure 7. A schematic representation of the cellular anatomy of the peripheral olfactory system of vertebrates and of its odor-evoked electrical activity (Courtesy of V. Vodyanoy re-drawn from R. Gestland). ORNs lie in OE; the cilia on their dendrites bathed by mucus (mu). Patch clamp electrode E1 measures a whole cell current (shown in inset a). Saline electrode E2 measures the EOG (shown in inset b). Electrode E3. A metal electrode measures extracellular spike activity in single receptor cell (shown in insets c and d). Bipolar wire electrodes E4 record spike activity from a bundle of axons (shown in inset e). The signal can be rectified and summated with decay (S) to give a smoothed measure of evoked activity (shown in inset f). Axon terminals branch at the olfactory bulb in glomeruli (GLOM, where they synapse with second order neurons). Electrode E5 is a saline pipette which records bulb surface potentials (shown in inset g). A microelectrode E6 records extracellular activity of single second order neurons (shown in inset h). The horizontal lines in insets b, c, e, g, and h represent the stimulus delivery period, 5 s. A whole cell current shown in inset a is evoked by an odorant pulse of 0.25 s. Inset d shows the extracellular action potential with calibration marks of 200 μ V and 5 ms.

2.8.1 Electroolfactogram

The electroolfactogram (EOG) is a measurement of the monophasic negative potential evoked by odors on the surface of multiple ORNs. The electroolfactogram is measured from the neuroepithelium in the nasal cavity, an area denoted by having a slightly yellow color as compared to the pink color of the respiratory epithelium (Figure 11 B).

Transduction of the odorant signal involves the production of local currents which produce the generator potential. The generator potential leads to generation of an action potential that travels through axons to secondary neurons in olfactory bulb. The EOG is characterized by a slow negative monophasic potential with a steep rising phase followed by an exponential fall towards the baseline following exposure of the olfactory epithelium to an odorant. The time course of the excitatory process therefore is a function of the number of odorant particles which reach the receptor per unit time and the time elapsing before the receptors become inactivated (Ottoson 1971).

There are multiple components of the EOG. The first is the rising phase, this due to the excitation of the olfactory receptors. The rising phase of the EOG output graph ascends to a peak level of activation. Next is the falling phase, as the line of the EOG begins to return to the baseline as a result of the elimination of stimulation particles (odorants).

The amount of time needed to accomplish this varies with the strength of the stimulus. Receptors stimulated by a weak odorant may require 1-2 seconds, while those activated by a stronger odorant may require 4-6 seconds. Once the potential has returned to the base line the receptors must recover in order to properly conduct the next olfactory signal, as they must regain their resting potential (Ottoson 1971).

2.8.2 EOG experiments.

There are two conventional methods to carry out EOG experiments. One method is carried out in situ, on the OE within the nasal cavity. In these experiments the animal is anesthetized, the roof of one nasal cavity is removed, and the OE exposed. An electrode consisting of a AgCl electrode, filled with saline solution, is contacted to the OE and measurements can be made (Gesteland, Lettvin et al. 1965; Scott and Scott-Johnson 2002). Irritation of the OE and the resulting production of mucus by the intact OE has been a problem associated with this method as it can attenuate signals from the OE. Another problem associated with this method is drying of the OE and the subsequent disconnection of the OE and electrode as the tissue desiccates and retreats from the electrode (Gesteland, Lettvin et al. 1965).

The other method is performed in vitro on intact epithelium after the epithelium is surgically removed. The EOG can still be recorded up to several hours after the animal has been euthanized and the tissue extracted. In our work we chose to surgically remove a fragment of olfactory epithelium (Chen, Lane et al. 2000; Sinnarajah, Dessauer et al. 2001; Grosmaître, Santarelli et al. 2007; Nickell, Kleene et al. 2007; Viswaprakash, Dennis et al. 2009). Since the OE is located in the caudal most aspect of the nasal cavity, surrounded by bone and vascularized tissue, it is a difficult location which to perform in situ experiments (Viswaprakash, Josephson et al. 2010). By removing a section of tissue for in vitro study we believe that we can have more control over the tissue in that we can control the amount of buffer in the perfusion chamber and prevent drying and the

production of copious amounts of mucus by the OE sample. Our method of odorant delivery is more like the natural sniffing process when odorant is delivered to the thin olfactory mucous layer with partially submerged olfactory cilia (Gesteland 1964; Ma, Chen et al. 1999).

2.9 Objectives and Specific Aims

We hypothesize that typical chemical compounds associated with explosives and explosive devices can activate rat olfactory receptors and that zinc nanoparticles can enhance the olfactory responses induced by these compounds.

The following specific aims will test the above hypothesis:

1. Prepare the rat olfactory epithelium fragments suitable for *in vitro* electroolfactogram (EOG) experiments.
2. Verify whether or not typical chemical compounds associated with explosives can induce EOG responses comparable with those elicited by conventional odorants.
3. Determine whether or not the tagging compound 2,3-dimethyl-2,3-dinitrobutane (DMNB), used to tag plastic explosives induces EOG responses.
4. Determine if zinc nanoparticles modulate EOG responses evoked by explosive odorants
5. Elucidate potential place of zinc nanoparticles action in the initial events of signal transduction.

Chapter 3.0 Materials and Methods

Animals of this project were cared by the Division of Laboratory Animal Health of the Auburn University. DLAH assures compliance with all applicable regulations. The primary regulations governing the care and use of animals used in research and teaching include the following: the Animal Welfare Act, the NIH-PHS Policy, the Guide for the Care and Use of Laboratory Animals, and the Guide for the Care and Use of Agricultural Animals in Agricultural Research and Teaching. The Division of Laboratory Animal Health maintains responsibilities in animal procurement, animal housing and daily care, the provision of veterinary care, health surveillance and preventative care, assisting investigators and their staff with animal procedures, and the care, maintenance and replacement of equipment and facilities. Accountability for all animals and facilities used for teaching and research is evaluated annually via an unannounced inspection by the USDA, APHIS, Animal Care Inspector.

3.1 Materials

3.1.1 Tools and materials for surgery

The list of tools and materials needed for rat olfactory epithelium slice preparation includes the following items: 1 gallon wide mouth plastic container, isoflurane, pentobarbital, laboratory guillotine, surgical microscope, scalpel, scissors/ fine scissors, rongeurs, and forceps.

3.1.2 Non explosive Odorants

All odorants were purchased from Sigma-Aldrich. An odorant mixture of ethyl butyrate, eugenol, and (+) and (-) carvone in water solution was investigated previously in rat EOG studies (Viswaprakash, Dennis et al. 2009; Viswaprakash, Josephson et al. 2010; Vodyanoy 2010). These odorants are not associated with explosives or their manufacture. In our work we refer to the solution of odorants not related to the manufacture of explosive as a standard odorant solution (SOS).

3.1.3 Explosive Odorants

The chemical compounds used in this study were chosen for their presence in manufacturing of many explosives: plasticizers and other components. These odorants are not explosive in nature, they are merely associated with the manufacturing process and present in the final explosive product. We refer to these odorants as explosive odorants merely for convenience. These odorants cover a large range of water solubility but have similar estimated concentration in olfactory mucus (Tables 1 - 3). We used a mixture of cyclohexanone, methyl benzoate, acetophenone and eugenol as these odorants are typically associated with explosives (Furton and Myers 2001; Jenkins, Leggett et al. 2001; Harper, Almirall et al. 2005; Kruse 2007; SWGDOG 2007). We refer the solution of explosive odorants dissolved in water as an explosive odorant solution (Mackay-Sim and Dreosti). Odorant mixtures were dissolved in pure water and the odorant vapors collected in the bottle headspaces were used as odor stimuli.

3.1.4 3-isobutyl-1-methylxanthine (IBMX)

IBMX is a membrane permeable phosphodiesterase inhibitor (Firestein, Darrow et al. 1991). It can produce olfactory neuron current without activation of olfactory receptors by functioning as a phosphodiesterase inhibitor that reduces the hydrolysis of cAMP produced by the olfactory receptor neurons. We used IBMX in order to produce a response from the ORN in the absence of an odorant. This was vital to our examination of the location of nanoparticle effects, as this allowed us to examine whether the nanoparticles enhance olfaction at the level of the CNG channels. Thus we could cut out the OR, G-protein, and AC and still the transduction cascade.

3.1.5 Preparation of epithelial slice

Male Sprague-Dawley rats were used in this work. The rat was placed in a plastic chamber along with the anesthetic isoflurane (Isoflo, ABBOT Laboratories). After an appropriate time, 0.5 ml of Pentobarbital Sodium Injection (Nembutal Sodium Solution) was administered intra -peritoneally. The rat was returned to its cage until its breathing slowed and movement ceased, at which point the rats were decapitated using a laboratory guillotine.

An incision was made along the dorsal midline of the head, while reflecting the tissue back on either side. The lower jaw was then removed using rongeurs in order to access the ventral aspect of the skull. Next the zygomatic arch and connecting temporal process and associated musculature were removed along with the eye using scissors and Ronguers. Ronguers were then employed to remove the caudal aspect of the frontal and

palatine bones, in order to expose the lateral side of the ethmoturbinates. These bones were removed past the midline on the dorsal aspect of the skull in order to access the ethmoturbinates from a dorsal approach. This is necessary in order to isolate the septum for removal without damaging the olfactory epithelium. A scalpel was used to cut through the ventral floor of the nasal mucosa and on either side of the dorsal portion of the nasal septum. Fine scissors were used to cut through the septum just rostral to the ethmoturbinates and along the caudal aspect of the turbinates along the length of the cribriform plate. The septum was then extracted using fine forceps and placed in a 60mm cell culture dish (Becton Dickinson) containing Hanks buffered saline solution with Ca^{+2} and Mg^{+2} .

After surgical removal and placement of the olfactory epithelial slice in a perfusion chamber, the tissue was stabilized for about 40 minutes until steady state EOG responses were achieved. The slice was viable and showed stable and reproducible behavior for ~ 2 hours. Partial submersion of the slice in the chamber relative to the buffer solution was important for a stable EOG recording. The tissue was kept wet but not fully immersed in solution. However, a dry mucus surface was not favorable to the generation of consistent EOG signals.

3.1.6 Zinc nanoparticles

Two sources of zinc nanoparticles were used in this work. First, they were prepared in our laboratory by electrolysis of solid zinc metal rods (Kruyt 1952). A homemade system was used that comprised a water container and a high voltage generator with 2 zinc metal

electrodes submerged in water. By controlling the voltage and distance between electrodes, the plasma created under water produces a very fine dispersion of metal nanoparticles. Two metal electrodes 2 mm in diameter were placed ~6 cm apart in a large pyrex jar 1mm below the air-water interface of 850 mL purified water that had been autoclaved at 23 psi and 120 °C and chilled to 25 °C. The jar was placed in a running water bath to prevent overheating. 15,000 V was applied across the electrodes for 12 hr. The Zn suspension was collected in a 1liter glass beaker and placed in a refrigerator for 12 hours so that large metal particles could sediment. The supernatant was transferred to tubes and centrifuged at 40,000×g for 90 min at 18 °C. The pellet was discarded after centrifugation. What remained was centrifuged two more times, with the final supernatant being subjected to analysis and particle counting. Time and speed needed to enrich nanoparticle suspensions smaller than 2 nm were estimated with the Stock's equation (Kruyt 1952).

A second colloidal zinc suspension was obtained from Purest Colloids, Inc. Suspensions were filtered through 0.22 µm syringe filters and centrifuged at 40,000×g for 90 min. UV absorption was used to estimate mean Zn nanoparticle concentrations, using a DU640 Beckman UV spectrophotometer. The centrifugation created a narrowing of the UV absorption bandwidth that indicated an increasing uniformity in nanoparticle size. The suspension was kept at 5 °C before use. Nanoparticle concentration is defined as the number of particles per liter of suspension. The number of particles per liter divided by Avogadro's number yields the molar particle concentration. Zinc nanoparticle

concentration was determined by particle counting and UV spectra analysis (Viswaprakash, Dennis et al. 2009).

3.2 Electroolfactogram

Our set up for electroolfactogram recording (Figures 8-15) is composed of a perfusion chamber contained in a Faraday box, pneumatic pico-pump, and devices for measuring and processing electrical signals.

A fragment of OE was placed in a perfusion chamber (Warner Instrument Corp., Hamden, CT) (Figures 10, 11) containing buffer (137 mM NaCl, 5.3 mM KCl, 4.2 mM NaHCO₃, 0.4 mM KH₂PO₄, 3.4 mM Na₂HPO₄, 5.6 mM D-glucose, 0.8 mM MgSO₄, and 1.2 mM CaCl₂ at pH 7.4). The tissue was positioned such that the lamina propria was immersed in the buffer, whereas the apical ciliated surface was exposed to air (Figure 11 B) and recordings were made at room temperature (25°C).

The EOG recording electrode, a Ag/AgCl wire in a glass pipette (Figure 11) of approximately 24 µm tip opening, was filled with the same physiological buffer then connected to an electronic amplifier to detect OE responses. The glass pipettes were fabricated using borosilicate capillaries (World Precision Instruments - WPI, Sarasota, FL) and pulled using a P-97 pipette puller (Sutter Instruments, Novato, CA). Once contact between the electrode and the OE surface was formed, odorant puffs were applied using air puffs generated by the picopump (section 3.4.1). Responses over a several minute time course were amplified by a 700A MultiClamp Amplifier (Axon Instruments), filtered at 2 - 5 kHz, and recorded.

The tissue in the chamber and microelectrode position were observed using an Hitachi digital camera with a long distance objective, LB50 Solaric Light source with a fiber optic cable, and monitor. The moment of contact between the electrode and the OE surface was detected by an OS 9020A GoldStar oscilloscope. The OE responses to stimuli were observed in real time with another monitor (Figure 9).

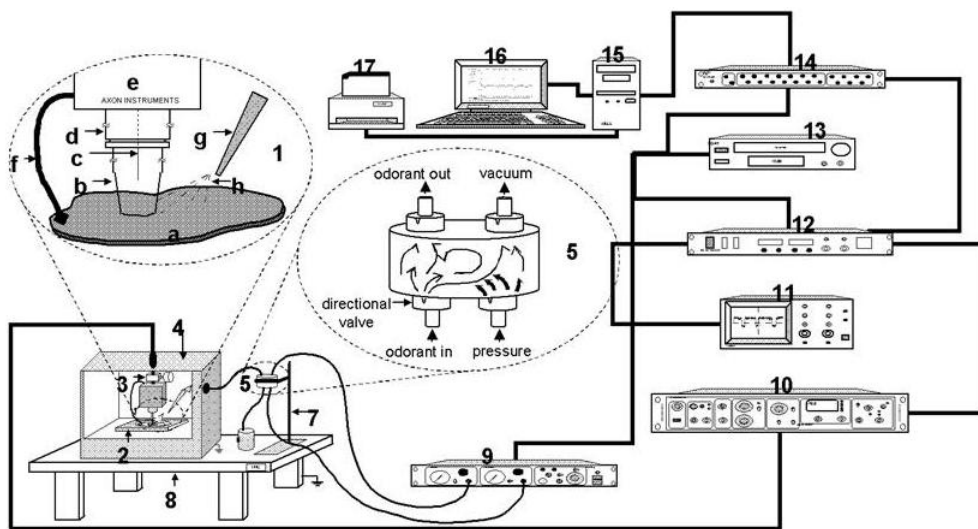


Figure 8. EOG setup: a. olfactory tissue; b. glass micro-electrode; c. silver/silver-chloride wire; d. glass micro-electrode holder; e. head stage; f. ground wire; g. odor applicator / puffer; h. odor stream, 2. Perfusion chamber, 3. Micro-manipulator, 4 Faraday-box, 5. Pressure regulator, 6. Liquid odorant container, 7. Metal stand, 8. Isolation table, 9. Pneumatic Pico-pump, 10. Patch-clamp amplifier, 11. Oscilloscope, 12. Analog-digital converter, 13. Video Cassette Recorder (VCR), 14. Digidata 1200A digital interface box 15. Computer CPU, 16. Computer monitor and keyboard, 17. Laser printer.

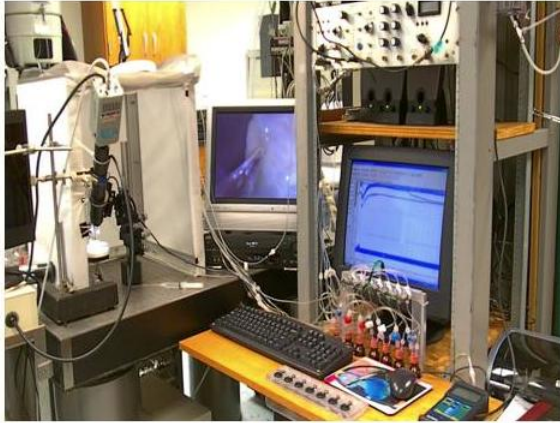


Figure 9. Experimental setup

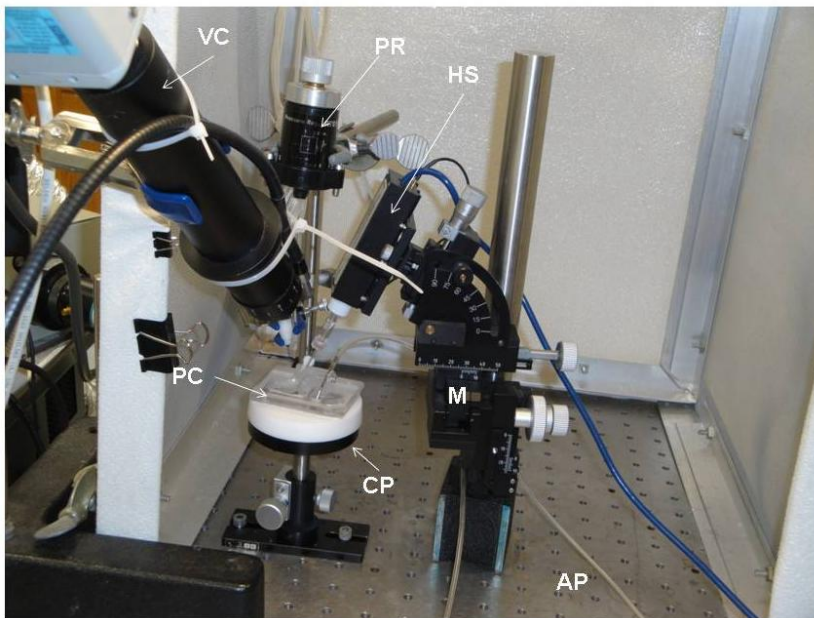


Figure 10. Close-up of EOG measurement system inside a Faraday box. PC – perfusion chamber, CP – perfusion chamber platform, HS – electronic head stage. M – 3D-micromanipulator, PR – pressure regulator, VC – video camera, AP – anti-vibration platform.

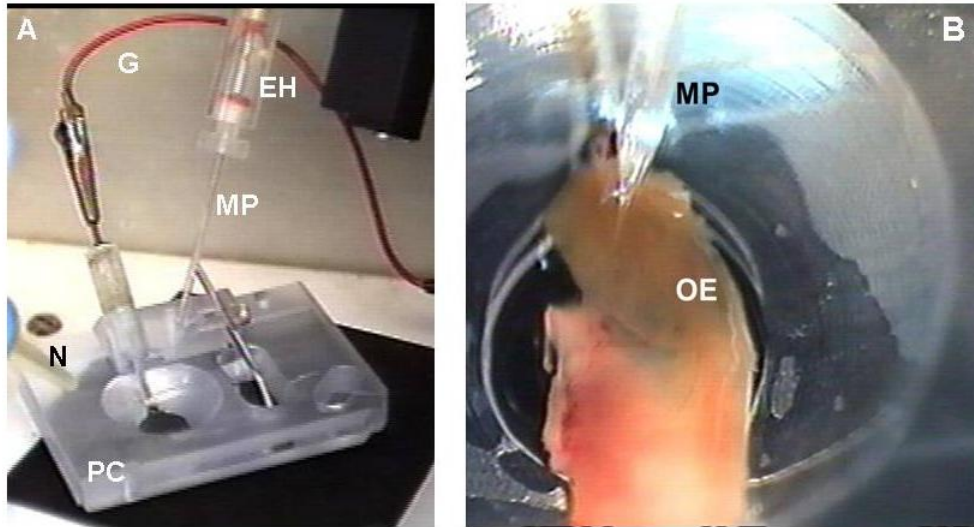


Figure 11. EOG measurement system. A. Perfusion chamber (PC). EH – electrode holder, MP – glass micropipette with Ag/AgCl electrode, G – ground wire, N – nozzle for odorant delivery. B. Fragment of olfactory epithelium (Schandar, Laugwitz et al.) is positioned on the bottom of the chamber well and partially immersed in a buffer solution, MP - glass micropipette with Ag/AgCl electrode. The olfactory epithelium is dark yellow (brownish).

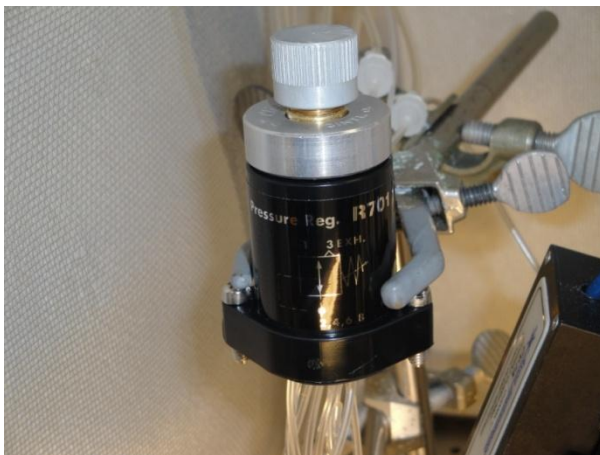


Figure 12 Pressure regulator. The regulator provides equal pressure for delivery of different odorants.

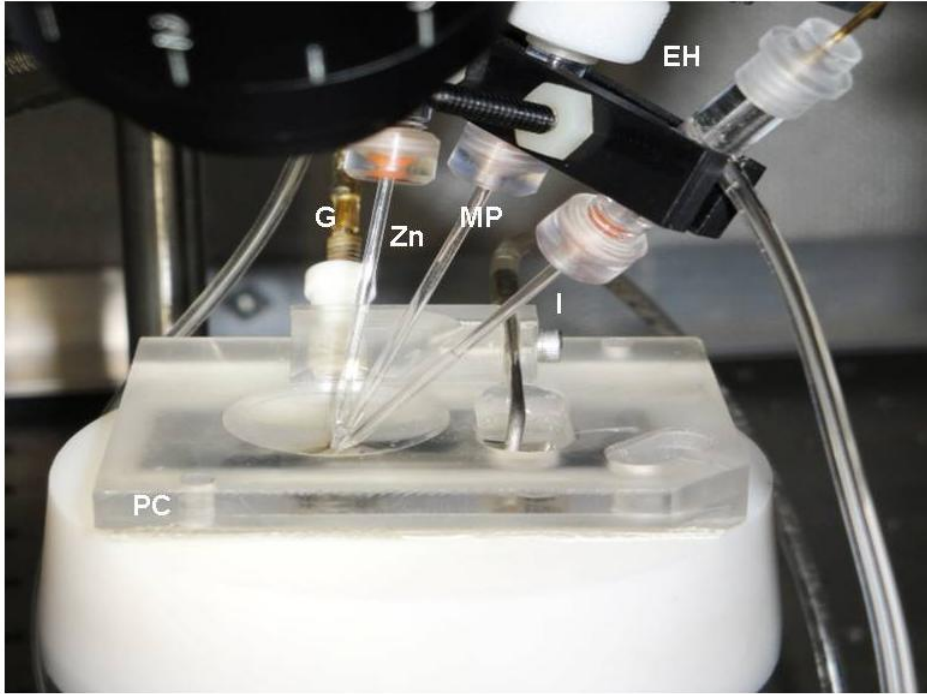


Figure 13. Perfusion chamber and electrode system for IBMX experiments. PC – perfusion chamber, MP – glass micropipette with Ag/AgCl electrode, I and Zn are glass micropipettes filled with IBMX solution and mixture of IBMX and zinc nanoparticles, respectively, G – ground wire, EH – electrode holder. Plastic tubes attached to micropipette holders deliver pulses of positive air pressure that drive liquid pulses out of pipette tips towards the olfactory epithelium.

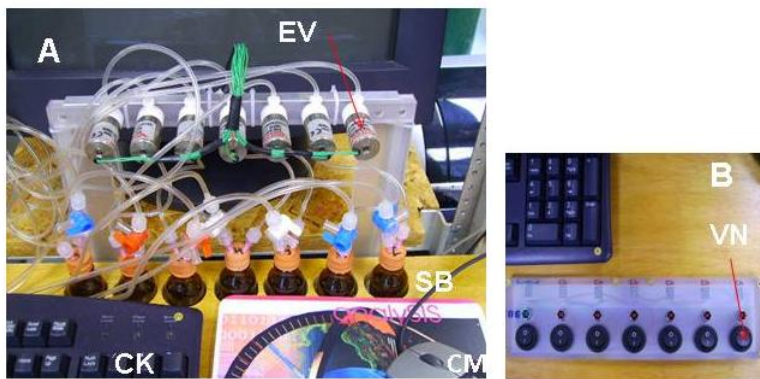


Figure 14. Valve control system. A – pneumatic valves. EV – one of the seven electric valves controlling stimuli delivery. SB – one of the seven stimuli bottles, containing solutions of odorants, chemical modulators, and suspension of zinc nanoparticles. CK and CM are computer keyboard and mouse, respectively. B – control board. VN – one of the seven control knobs operating electric valves.

3.3 Stability of EOG responses

Because of large variability of odorant responses by individual cells (Firestein, Picco et al. 1993), stability over an extended period and response reproducibility at a single contact were required. We made considerable efforts to correct mechanical and electrical problems that potentially could affect stability of the system. Pulses of the air and odorant flows used as EOG stimuli were precalibrated with ADM2000 Flowmeter (Krackeler Scientific Inc) so that the relative change in the amplitude of two consecutive stimuli was less than 1% (Viswaprakash, Josephson et al. 2010). The perfusion chamber was contained in a grounded Faraday box on a vibration isolation table (GS-34 Newport) (Figures 9-10). Experiments were carried out at 25 ± 4 °C and 50 ± 5 % of relative humidity. The glass nozzle for air/odorant delivery and measuring electrode were mounted on the Soma MX1100 R High Precision Micromanipulator providing reproducible direction and position of the nozzle and electrode (Figure 10). Electronically controlled valves were used to control odorant delivery (Figure 14-15). Unique delivery devices for IBMX and DMNB were also used in our set up (Figures 12-13). Finally, we incorporated a digital video camera and monitor that allowed precise visual control of microelectrode contact with olfactory tissue.

3.4 Delivery of stimuli

3.4.1 Odorant delivery

For stimulation, a 0.25 s pulse of the odorant mixture (SOS or EOS) at 8 psi was formed by a computer controlled Pneumatic PicoPump PV800 (World Precision Instr.). A pulse

of positive pressure drove the odorant into a calibrated multibarrel pipette fitted with a glass nozzle directed at the OE (Figure 11). Each pipette barrel could pass a puff of distinct odorant composition and concentration. The residual odorant was cleared by air between each stimulus application. The odorant pulse patterns were initiated manually at predetermined time intervals or automatically by computer. The automatic computer routine was composed of ten 0.25 s pulses of 8 p.s.i at 20 s intervals. Thus one series of ten pulses at 20 s intervals constituted one “EOG recording”. Thus the single “EOG recording” had a duration of 200 s and correspond to 10 response traces.

The odorant concentration that is actually experienced by the OE receptors can be estimated from the mucus/air molar partition coefficient that is in a range of 10^{-10} to 10^3 (Amoore and Buttery 1978). Considering values of water/air partition coefficients, the concentrations of odorants in the mucus can be estimated to be one to three orders of magnitude lower than the solution concentrations (Zhou, Illies et al. 1993; Araneda, Kini et al. 2000). Taking the average values of the water/air and mucus/air partition coefficients as 10^{-3} and 10^2 respectively, we estimate that the EOG dose-dependency relationship was saturated around $\sim 10 \text{ mM} \times 10^{-3} \times 10^2 = 1 \text{ mM} = 1000 \text{ }\mu\text{M}$ (Viswaprakash, Dennis et al. 2009; Viswaprakash, Josephson et al. 2010)

3.4.2 Zinc nanoparticle delivery

A nanoparticle suspension was mixed with odorant solutions. During the puff, the odorant vapor containing zinc nanoparticles was delivered to the OE surface. In the case of IBMX experiments (see below), zinc nanoparticles were mixed with IBMX.

3.4.3 IBMX delivery

Micropipettes, labeled I and Zn (Figure 13) were filled with IBMX dissolved in buffer solution and IBMX solution + zinc nanoparticles, respectively. After the microelectrode (Figure 13, MP) forms a stable contact with OE, a 0.25 s pulse of IBMX or IBMX+Zn was delivered to the vicinity of this contact. We used 400 μ M IBMX solution to evoke an EOG response. It was demonstrated that IBMX at this concentration can excite rat olfactory receptor neurons (Ma, Chen et al. 1999).

3.3.4 DMNB delivery

Unlike our SOS and EOS solutions we were not able to make a stable water solution of DMNB. Therefore, instead of producing DMNB vapors from solutions we generated vapors by sublimation of the solid crystalline compound. The DMNB vapor applicator is composed of two glass compartments separated by a fine glass filter (Figure 15). The crystalline DMNB compound is placed in the upper compartment on the filter. The upper compartment is connected by a tube with a nozzle directed towards OE, while the lower compartment is coupled with an air pressure system. As the DMNB sublimates the vapor is collected in the upper compartment. A 0.25 s pulse of air from the picopump applied to the lower compartment sends the vapor pulse to the nozzle and OE.

DMNB sublimates and produces 2.7 ppm vapor (BCST 1998). The smallest concentration detectable by a canine, or the dog's low odor detection (Minic, Persuy et al.) level for the explosive compounds used in this work is around a few ppb (Table 2).

Thus, concentration of DMNB was ~1000 times higher than LOD of the explosive odorants.



Figure 15. Odorant applicators for DMNB. The applicator allows delivering sublimation vapors from a solid DMNB (Courtesy of P. Waggoner)

3.5 Modulation of EOG responses by zinc nanoparticles

EOG responses to compounds related to explosives (“explosive odorants”) were compared to those produced by the same odorants in the presence of zinc nanoparticles. When triggered either manually or by the software, the Pico pump sent a puff of air down a tygon tube. The air traveled down the main tube to a series of seven electronic valves, six of which controlled tubes that entered into bottles containing odorant, the seventh led directly to the epithelium in the perfusion chamber. The tubes traveling to odorant bottles ended in a hypodermic needle that penetrated the rubber diaphragm of a bottle containing odorant solution. The puff of air carried the head space odorant vapor to olfactory epithelium, thereby stimulating the olfactory neurons. The seventh tube with clean air from the picopump was used both as a control and for clearing the OE between odorant pulses. This setup enabled us to study the effects of zinc nanoparticles on electrical

responses generated by explosive odorants. Half of the bottles contained only odorant, the other half contained the odorant plus zinc nanoparticles.

3.6 Localization of zinc nanoparticle action

An odorant induced olfactory response includes a complicated cascade of initial biochemical events (Figure 6). A sensory transduction includes three major steps: (1) odorant binding to the receptor-G-protein complex and release of α -G-protein subunit; (2) activation of adenylyl cyclase and generation of cAMP, and (3) a cAMP activation of ion currents that are manifested by EOG response. Zinc nanoparticle enhancement could occur at any of the these locations

3.7 Data development

Data development, or the production of EOG graphs, was performed by using pCLAMP Electrophysiology Data Acquisition and Analysis Software (Molecular Devices) and Origin Software (Mictocal).

Chapter 4.0 Results

4.1 Stability and repeatability of olfactory responses

Approximately ten electrode/OE contacts and several recordings were made in the majority of experiments with explosive odorants. We were successful in roughly 70% of contacts in obtaining 10 response traces per recording. The mean value of the relative change of 2 consecutive EOG peaks stimulated by the same odorant pulse was 5%. The electronic noise observed in the system in most cases did not exceed a few percent of the overall signal.

4.2 Standard odorant solution with zinc nanoparticles

Before beginning experiments with the explosive odorant solutions (Mackay-Sim and Dreosti) we reproduced the zinc nanoparticles effect observed by Viswaprakash and colleagues (Viswaprakash, Dennis et al. 2009) with standard odorant solution (SOS). A typical EOG response to the conventional odorant pulses are shown in Figure 16. This figure represents ten electrode contacts, each with ten sequential applications of stimuli. When olfactory neurons were excited by a standard odorant solution (SOS) mixed with zinc nanoparticles, the EOG odorant response was significantly increased.

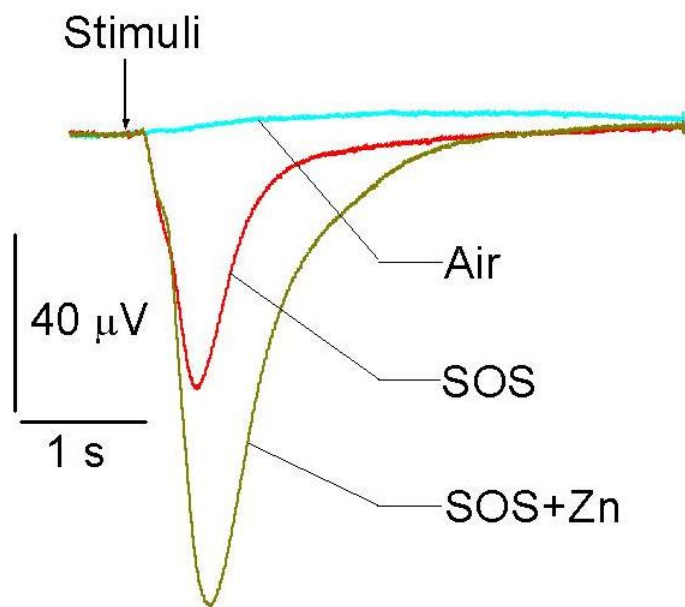


Figure 16. EOG traces recorded from rat olfactory epithelium. EOG recording of odor induced responses. The responses were induced by air, standard odorant solution (SOS), and SOS with zinc nanoparticles (SOS+Zn). The arrow indicates time at which 0.25 s stimuli were applied. The figure shows representative traces of 10 electrode contacts with the OE, with each contact 10 sequential stimuli were applied. These pulses alternated between applying purified air (control), back space vapors above a 16 mM standard odorant solution, and back space vapors above that same solution with 1.4 nM Zn nanoparticles.

4.3 Explosive odorant solution with zinc nanoparticles

Figure 17 shows an EOG evoked by 16 mM EOS and EOS+5.6 nM zinc nanoparticles.

The odorant vapors from the head space of bottles containing EOS compounds with and without zinc nanoparticles were delivered by the system shown in Figure 11. The data show an almost three fold increase of the response magnitude.

We increased the zinc nanoparticle concentration in a stepwise manner beginning with 0.5 nM then increasing to 1.4 nM, 2.82 nM, 4.2 nM, and 5.6 nM Zn. Each increase in zinc nanoparticle concentration generated an increase in odorant induced response from the

neuron (Figure 18). Therefore, the observed effect of zinc nanoparticles is dose dependent.

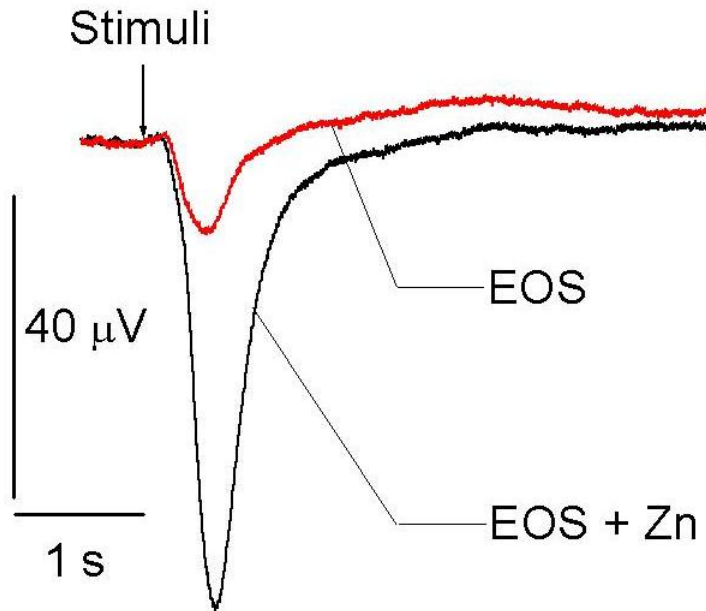


Figure 17. Zinc nanoparticles enhance EOG responses induced by odorants related to the manufacture of explosives. EOS and EOS+Zn are typical traces generated by a 0.25 s pulse of the back space vapors above the 16 mM explosive odorant solution and EOS with 5.6 nM zinc nanoparticles, respectively. The traces are representative of 3 tissues and 28 recordings.

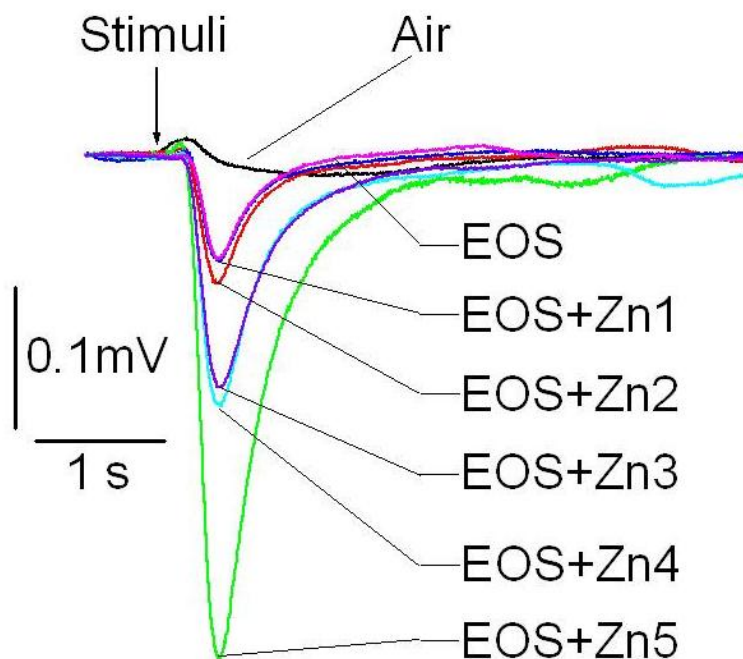


Figure 18. EOG traces induced by vapors of explosive odorant solutions with varying concentrations of zinc nanoparticles. EOS = 8 mM explosive odorant solution, Zn nanoparticle concentrations are Zn1-Zn5= 0.6, 1.4, 2.8, 4.3, 5.6 nM respectively. The figure represents typical responses obtained from 4 tissues and 35 recordings.

4.4 Taggant: DMNB (2,3-Dimethyl 2,3-Dinitrobutane)

Figure 19 shows EOG responses evoked by a the taggant compound DMNB (2,3-Dimethyl 2,3-Dinitrobutane) in comparison to air and SOS evoked responses. The response generated by the SOS reached a maximum of 100 μ V over the course of one second. The EOG response from DMNB was not different from the one induced by air. This demonstrates that the DMNB is not detected by OE. The figure represents the response from 3 different OE tissue samples and a total of 23 recordings.

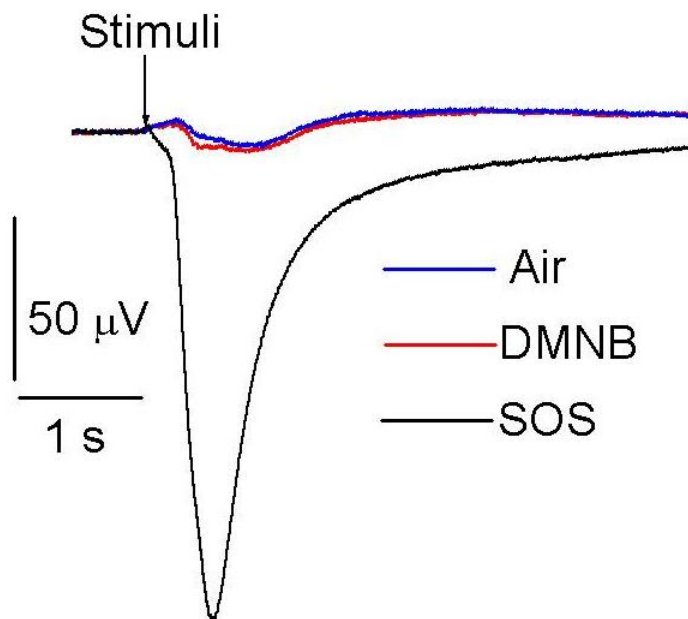


Figure 19. EOG responses to a taggant, DMNB, and standard odorant solution. EOG responses were induced by air and vapors from DMNB and standard odorant solution (SOS). The DMNB vapor was delivered by the odorant applicator shown in Figure 15, while SOS vapor was applied through the nozzle system (Figure 11). SOS represents a 0.25 s vapor pulse of a 16 mM standard odorant solution, and DMNB is a pulse of the same longevity, but produced by the sublimation vapor of solid DMNB powder. The figure shows representative traces obtained from 3 tissues and 23 recordings.

4.5 Comparison of explosive and standard odorants

After observing the response for both standard and explosive odorant without zinc, it appeared that the amplitude of response for explosive odorants was much smaller than that of the standard odorants. The vapor of pure water was used as a control (Figure 20). The response generated by SOS reached a maximum of over 40 μV . The response from EOS failed to reach half that of the SOS, while EOS did generate a response greater than that of air. These results demonstrate that the odorants associated with the manufacture of explosives, that we chose, are not detected by dissected OE to the same degree as other odorants.

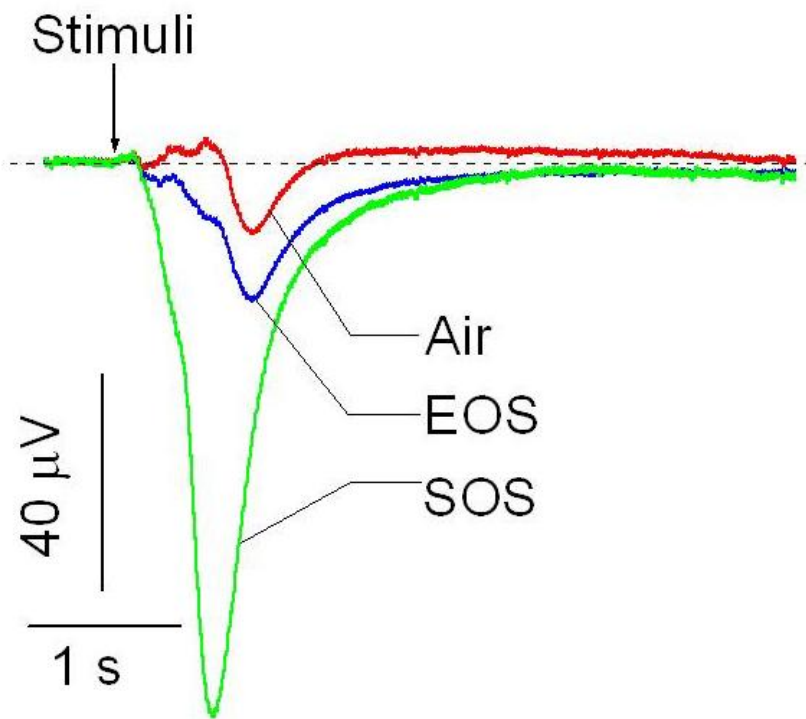


Figure 20. Comparison of EOG responses induced by the standard and explosive odorants. EOG responses induced by a 0.25 s vapor pulse of purified water (Adamek, Gesteland et al.), 16 mM explosive odorant solution (Mackay-Sim and Dreosti), and 16 mM standard odorant solution (SOS). The vapors are applied through the nozzle system (Figure 11). The figure represents data obtained from 3 tissues and 26 recordings.

4.6 Location of zinc nanoparticle action

IBMX is a membrane permeable phosphodiesterase inhibitor (Firestein, Darrow et al. 1991). It can produce olfactory neuron current without activation of olfactory receptors. As a phosphodiesterase inhibitor, it reduces the hydrolysis of cAMP produced by the olfactory receptor neurons, thereby allowing ambient cAMP levels to activate the CNG channels. Using IBMX together with zinc nanoparticles, we can determine whether or not zinc nanoparticles can modulate ORN responses without activation of olfactory receptors. If zinc nanoparticles could modulate olfactory responses induced by IBMX, then it would indicate that later steps of signal transduction are involved in zinc effects. On the other

hand, if zinc nanoparticles could not affect IBMX induced olfactory response, it would mean that zinc is involved in the earlier steps of transduction.

In preliminary experiments, we dissolved IBMX in water and attempted to induce olfactory responses by applying pulses of water vapor carrying IBMX molecules. However, we were not able to produce noticeable OE responses to IBMX, because of the low air/water distribution coefficient. Therefore, we constructed a special system for IBMX and zinc nanoparticle delivery in buffer solution. The buffer, functioning as the control, did not generate a response from OE. IBMX alone generated a response of 0.08 mV over a one second period of time. This is similar to the odorant induced response. Therefore we were able to demonstrate that the OE can generate a response from IBMX without the application of odorants (Figure 21). IBMX generated a peak response of 0.08mV without zinc nanoparticles. When the zinc nanoparticles were added to the IBMX solution the response was indistinguishable from that of the IBMX alone (Figure 22). There was no significant difference between olfactory responses to IBMX alone and IBMX+Zn nanoparticles.

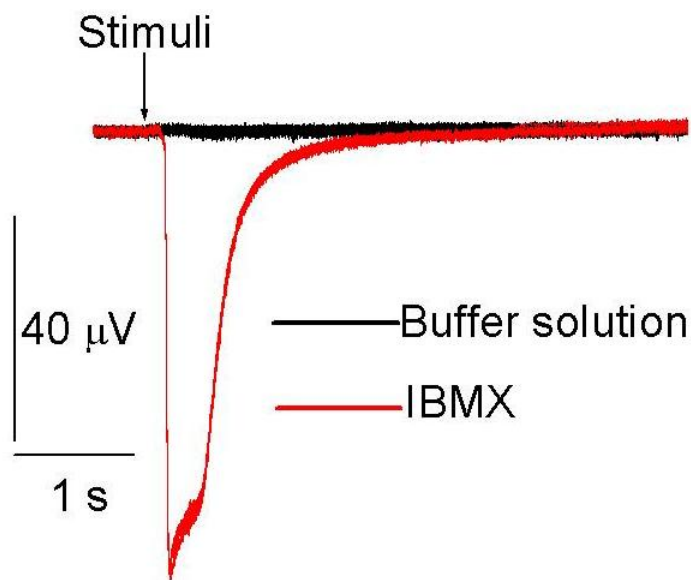


Figure 21. EOG response evoked by IBMX. EOG response induced by 0.25 s pulse of 400 μM IBMX without odorant. The 0.25 s pulse of buffer solution is applied as a control. Both IBMX and control pulses are applied by injection from micropipettes filled with 400 μM IBMX and buffer solution, respectively. The stimuli application is carried out by the electrode system shown in Figure 12. The figure shows representative traces from 3 tissues and 21 recordings.

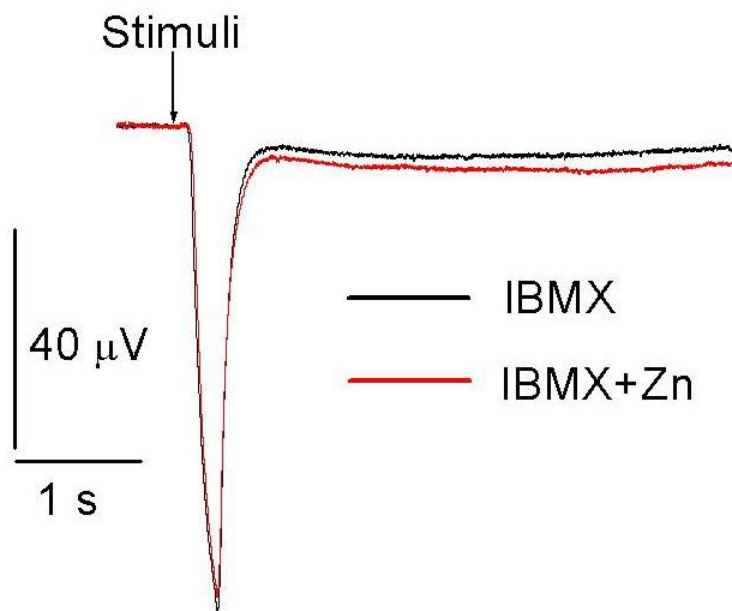


Figure 22. Zn nanoparticles do not enhance EOG responses induced by IBMX. EOG response induced by 0.25 s pulse of 400 μM IBMX with and without zinc nanoparticles. The 0.25 s pulses are applied by injection from micropipettes filled with 400 μM IBMX and 400 μM IBMX + 4 nM zinc nanoparticles, respectively. The stimuli applications are carried out by the electrode system shown in Figure 13. The figure shows representative traces from 3 tissues and 25 recordings.

Chapter 5.0 Discussion

Our method of preparing the OE sample for in vitro study provides greater stability in that we are able to control the cellular environment. By preparing the tissue in this way we can control the buffer solution in which the tissue is bathed, ensuring that there are no divalent cations that could interfere with our results and preventing desiccation of the tissue or over production of mucus by an intact OE. We believe this method of tissue preparation has enabled us to achieve more homogenous results.

The stability of the slide and ability to produce reproducible EOG responses (section 3.3) were consistent with those obtained by other researchers (Chen, Lane et al. 2000; Sinnarajah, Dessauer et al. 2001; Grosmaître, Santarelli et al. 2007; Nickell, Kleene et al. 2007; Viswaprakash, Dennis et al. 2009). We used vapor taken from the bottle head space above odorant solutions and puffed the vapor over the surface of partially submerged OE. Some investigators (Pinato, Rievaj et al. 2008) applied odorant directly to the ORNs in a bath solution submerging their OE sample. Our method of odorant delivery is similar to the natural sniffing process where the odorant is delivered to the thin olfactory mucous layer with partially submerged olfactory cilia.

We used a mixture (EOS) of cyclohexanone, methyl benzoate, acetophenone and eugenol, typical explosive odorants (Furton and Myers 2001; Jenkins, Leggett et al. 2001; Harper, Almirall et al. 2005; Kruse 2007; SWGDOG 2007). We verified that these

odorants associated with explosives and explosive devices can induce EOG responses. After observing the response for both standard and explosive odorant it appeared that the amplitude of response for explosive odorants was much smaller than that of the standard odorants. These results agree well with the recent work by (Corcelli, Lobasso et al. 2010). After studying six chemical compounds associated with explosives and explosive devices they were able to activate rat olfactory receptors using an EOG. Compared to the EOG signal produced by amyl acetate, a conventional odorant, the EOG responses measured by Corcelli and colleagues to phenol, naphthalene, hexachloroethane, benzothiazole, diphenylamine, benzene, toluene, styrene, and chlorobenzene were smaller. The explosive odorants we used together with the compounds analyzed by Corcelli et al represent 10 explosive odorants that generate measurable EOG responses and make them potentially useful for canine detection (Doty, Kreiss et al. 1990; Corcelli, Lobasso et al. 2010). Due to the small response the EOG amplitudes evoked by explosive odorants, it may be desirable to enhance the response amplitude from these odorants, in order to ensure their detection.

We demonstrated that the odorant induced response initiated by odorants related to the manufacture of explosives was dramatically enhanced by zinc nanoparticles. We estimated that total exposure of searching dogs to zinc nanoparticles from “sniffing samples” was calculated to be on the order of 5 micrograms zinc (expressed as total zinc) per animal/day. This level of exposure is 2100 times less than US Government standards for Minimal Risk Levels (MRL) for zinc. Therefore we speculate that the concentration

of zinc nanoparticles is very low and therefore it may be considered safe to use with live animals.

DMNB is the preferred taggant in the United States and is stated to be detectable at 0.5 parts per billion (ICAO 1991; Jones, Augsten et al. 1995; BCST 1998). In our experiments the EOG response from 2.7 parts per million DMNB was not different from that induced by the air. Therefore DMNB at more than 5000 times higher concentration than the supposed detectable concentration does not generate a measurable EOG response. Additionally, field tests with trained detector canines have indicated that DMNB may not be detectable by these animals (Furton and Myers 2001; Harper, Almirall et al. 2005). These facts are of great significance as DMNB, as a taggant, is incorporated into explosives in order to ensure their detection. Thus, our results have not shown that DMNB is effective as a taggant and its use as such should be closely reexamined. More research is needed both with isolated neurons and detector dogs to fully evaluate DMNBs usefulness as a tagging compound.

We were able to generate an EOG response without activation of olfactory receptors by using IBMX, a phosphodiesterase inhibitor that reduces the hydrolysis of cAMP produced by the ORN. We further demonstrated that zinc nanoparticles do not affect the IBMX-induced olfactory response. Therefore, zinc nanoparticles do not enhance at the level of the ion channels, suggesting zinc is involved in earlier steps of signal transduction. We suggest that in the future, additional experiments be carried out with

other pharmacological agents that increase cytoplasmic cAMP and activate the later stages of the transduction cascade.

The mechanism by which zinc nanoparticle enhancement occurs is not clear. It has been speculated that these zinc nanoparticles could act as a “mini battery”. In this model, the zinc nanoparticles are bound to the mucosal side of the membrane (Ball 2009; Vodyanoy 2010). Some of the zinc atoms from the nanoparticles spontaneously go into solution as Zn^{2+} ions and leave behind electrons (Vodyanoy 2010). These ions could then take part in Turin’s model of OR function, where an electron is transferred to a zinc ion that then breaks the disulfide bond between receptor and G-protein.

However, these nanoparticles lack any charge and can therefore quickly diffuse into the cell without the aid of ion channels, within 90-800 μs (Viswaprakash, Dennis et al. 2009). Using transmission electron microscopy the nanoparticles were observed on the cytoplasmic side of the ORN membrane. Once inside the cell, the nanoparticles could exert their modulatory effects on a different portion of the olfactory signal transduction pathway. This ability to quickly diffuse into the cell does not mean that their effect is not associated with the OR- G_{olf} complex. It was observed that the latency between stimulus arrival and onset of current is no longer than 160 ms (Grosmaître, Vassalli et al. 2006), therefore these nanoparticles are not diffusing very far (Viswaprakash, Dennis et al. 2009) before they enhance the odor induced response. Furthermore, since no enhancement was observed while using IBMX, and that the enhancement only occurs with the combination of odorant and zinc nanoparticles, the site of action could be the OR- G_{olf} complex.

Further testing is needed to properly isolate the site of zinc nanoparticle enhancement. Perhaps using a known adenylyl cyclase activator, such as Forskolin, could provide useful information as to the location of zinc nanoparticle enhancement of the odorant induced response of the ORN. Using Forskolin could remove the OR and G_{olf} from the signal pathway, much the same way that using IBMX essentially removes everything before the CNG channels in the olfactory transduction pathway. Enhancement seen with Forskolin would suggest that enhancement is occurring at the level of ACIII or that perhaps enhancement is occurring at both the OR- G_{olf} complex and at ACIII. However, if enhancement is not seen with Forskolin it could indicate that the enhancement is occurring at the level of the OR- G_{olf} complex.

In our work we used rats as a model to study the explosive odorant induced EOG response. Our long term objective is to enhance canine detection of explosive odorants; however, further study using canine OE is necessary to achieve this objective. The results of this work can be used for further studies of other chemical compounds and future practical use of metal nanoparticle enhancement of canine odorant detection.

Chapter 6.0 Conclusions

1. We prepared the rat olfactory epithelium fragments suitable for in vitro electroolfactogram (EOG) experiments. The slices were viable and showed stable and reproducible behavior for ~ 2 hours.
2. We verified that our mixture of four typical chemical compounds associated with explosives can induce EOG responses and compared these responses with those elicited by conventional odorants.
3. We determined that zinc nanoparticles strongly enhance EOG responses evoked by explosive odorants.
4. We determined that the tagging compound 2,3-dimethyl-2,3-dinitrobutane (DMNB), used to tag plastic explosives, does not induce EOG responses at concentration of 2.7 ppm in air.
5. We determined that zinc nanoparticles do not enhance an olfactory response to odorant at the CNG-channel level and that zinc is involved in the earlier steps of signal transduction.

References

- Abraham, M. H., J. M. R. Gola, et al. (2002). "A model for odour thresholds." Chemical Senses **27**(2): 95-104.
- Ache, B. W. and J. M. Young (2005). "Olfaction: Diverse species, conserved principles." Neuron **48**(3): 417-430.
- Adamek, G. D., R. C. Gesteland, et al. (1984). "Transduction Physiology of Olfactory Receptor Cilia." Brain Research **310**: 87-97.
- Adams, D. R. (1972). "Olfactory and non-olfactory epithelia in the nasal cavity of the mouse, *Peromyscus*." American Journal of Anatomy **133**(1): 37-49.
- Aedo, F., R. Delgado, et al. (2007). "Copper and zinc as modulators of neuronal excitability in a physiologically significant concentration range." Neurochemistry International **50**(4): 591-600.
- Aiken, J. D. and R. G. Finke (1999). "A review of modern transition-metal nanoclusters: their synthesis, characterization, and applications in catalysis." Journal of Molecular Catalysis a-Chemical **145**(1-2): 1-44.
- Alexander, T. H. and T. M. Davidson (2006). "Intranasal zinc and anosmia: The zinc-induced anosmia syndrome." Laryngoscope **116**(2): 217-220.
- Allison, A. C. (1953). "The morphology of the olfactory system in the vertebrates." Biological Reviews of the Cambridge Philosophical Society **28**(2): 195-244.
- Allison, A. C. and R. T. T. Warwick (1949). "Quantitative observations on the olfactory system of the rabbit." Brain **72**(2): 186-&.
- Amoore, J. E. (1963). "Stereochemical Theory of Olfaction." Nature **199**(4896): 912-913.
- Amoore, J. E. (1964). "Current status of the steric theory of odor." Annals of the New York Academy of Sciences **116**(2): 457-476.
- Amoore, J. E. and R. G. Buttery (1978). "Partition-Coefficients and Comparative Olfactometry." Chemical Senses & Flavour **3**(1): 57-71.
- Anholt, R. R. H. (1989). "Molecular Physiology of Olfaction." American Journal of Physiology **257**(6): C1043-C1054.
- Anholt, R. R. H. (1994). "Signal integration in the nervous-system- adenylyl cyclasees as molecular coincidence detectors." Trends in Neurosciences **17**(1): 37-41.
- Araneda, R. C., A. D. Kini, et al. (2000). "The molecular receptive range of an odorant receptor." Nature Neuroscience **3**(12): 1248-1255.
- Bakalyar, H. A. and R. R. Reed (1990). "Identification of a Specialized Adenylyl Cyclase That May Mediate Odorant Detection." Science **250**(4986): 1403-1406.
- Ball, P. (2009) "Column: The crucible." Advancing the Chemical Sciences; Chemistry World
- BCST (1998). Containing the Threat from Illegal Bombings: An Integrated National Strategy for Marking, Tagging, Rendering Inert, and Licensing Explosives and Their Precursors Explosives and Their Precursors. Washington, D.C., National Academy Press.
- Blanton, M. G., J. J. Lo Turco, et al. (1989). "Whole cell recording from neurons in slices of reptilian and mammalian cerebral cortex." Journal of Neuroscience Methods **30**(3): 203-210.

- Bonigk, W., W. Altenhofen, et al. (1993). "Rod and cone photoreceptor cells express distinct genes for cGMP-gated channels." Neuron **10**(5): 865-877.
- Boudjelal, M., A. Sivaprasadarao, et al. (1996). "Membrane receptor for odour-binding proteins." Biochemistry Journal **317**: 23-27.
- Breer, H. (2003). "Olfactory receptors: molecular basis for recognition and discrimination of odors." Analytical and Bioanalytical Chemistry **377**(3): 427-433.
- Breer, H., J. Fleischer, et al. (2006). "The sense of smell: multiple olfactory subsystems." Cellular and Molecular Life Sciences **63**(13): 1465-1475.
- Breipohl, W. (1972). "Licht- und elektronenmikroskopische Befunde zur Struktur der Bowmanschen Drüsen im Riechepithel der weißen Maus." Cell and Tissue Research **131**(3): 329-346.
- Brennan, P. A. and F. Zufall (2006). "Pheromonal communication in vertebrates." Nature **444**(7117): 308-315.
- Brookes, J. C., F. Hartoutsiou, et al. (2007). "Could Humans Recognize Odor by Phonon Assisted Tunneling?" Physical Review Letters **98**(3): 038101.
- Brown, D., L. M. Garcia-Segura, et al. (1984). "Carbonic anhydrase is present in olfactory receptor cells." Histochemistry and Cell Biology **80**(3): 307-309.
- Brunet, L. J., G. H. Gold, et al. (1996). "General anosmia caused by a targeted disruption of the mouse olfactory cyclic nucleotide-gated cation channel." Neuron **17**(4): 681-693.
- Buck, L. and R. Axel (1991). "A novel multigene family may encode odorant receptors - a molecular-basis for odor recognition." Cell **65**(1): 175-187.
- Buck, L. and R. Axel (1991). "A novel multigene family may encode odorant receptors: a molecular basis for odor recognition." Cell **65**(1): 175-87.
- Buck, L. B. (2004). "Olfactory Receptors and Odor Coding in Mammals." Nutrition Reviews **62**(11): S184-S188.
- Buck, L. B. (2005). "Unraveling the Sense of Smell (Nobel Lecture)." Angewandte Chemie International Edition **44**(38): 6128-6140.
- Buiakova, O. I., H. Baker, et al. (1996). "Olfactory marker protein (OMP) gene deletion causes altered physiological activity of olfactory sensory neurons." Proceedings of the National Academy of Sciences of the United States of America **93**(18): 9858-9863.
- Caggiano, M., J. S. Kauer, et al. (1994). "Globose basal cells are neuronal progenitors in the olfactory epithelium: A lineage analysis using a replication-incompetent retrovirus." Neuron **13**(2): 339-352.
- Carr, V. M., S. P. Murphy, et al. (1994). "Small subclass of rat olfactory neurons with specific bulbar projections is reactive with monoclonal-antibodies to the HSP70 heat shock protein." Journal of Comparative Neurology **348**(1): 150-160.
- Carr, V. M., E. Walters, et al. (1998). "An enhanced olfactory marker protein immunoreactivity in individual olfactory receptor neurons following olfactory bulbectomy may be related to increased neurogenesis." Journal of Neurobiology **34**(4): 377-390.
- Case, L. P. (2005). The Dog's Body. Ames, Iowa, Blackwell Publishing Professional.
- Chen, S., A. P. Lane, et al. (2000). "Blocking Adenylyl Cyclase Inhibits Olfactory Generator Currents Induced by "IP3-Odors"." J Neurophysiol **84**(1): 575-580.

- Coates, E. L. (2001). "Olfactory CO₂ chemoreceptors." Respiration Physiology **129**(1-2): 219-229.
- Connolly, J. M., W. A. Curby, et al. (1998). Detection of Hidden Explosives. Forensic investigation of explosions. A. Beveridge. London, Taylor and Francis Ltd: 62.
- Corcelli, A., S. Lobasso, et al. (2010). "Detection of explosives by olfactory sensory neurons." J Hazard Mater **175**(1-3): 1096-100.
- Costanzo, R. M. (1985). "Neural Regeneration and Functional Reconnection Following Olfactory Nerve Transection in Hamster." Brain Research **361**: 258-266.
- Costanzo, R. M. and E. E. Morrison (1989). "3-dimensional scanning electron-microscopic study of the normal hamster olfactory epithelium." Journal of Neurocytology **18**(3): 381-391.
- Doty, R. L., D. S. Kreiss, et al. (1990). "Human Odor Intensity Perception - Correlation with Frog Epithelial Adenylate-Cyclase Activity and Transepithelial Voltage Response." Brain Research **527**(1): 130-134.
- Doucette, R. (1993). "Glial cells in the nerve fiber layer of the main olfactory bulb of embryonic and adult mammals." Microscopy Research and Technique **24**: 113-130.
- Eng, D. L. and J. D. Kocsis (1987). "Activity-dependent changes in extracellular potassium and excitability in turtle olfactory nerve." Journal of Neurophysiology **57**(3): 740-754.
- Firestein, S. (2001). "How the olfactory system makes sense of scents." Nature Reviews **413**: 211-218.
- Firestein, S. (2001). "How the olfactory system makes sense of scents." Nature **413**(6852): 211-218.
- Firestein, S., and Frank Zufall (1994). "The cyclic nucleotide gated channel of olfactory receptor neurons." Cell Biology **5**: 39-46.
- Firestein, S., B. Darrow, et al. (1991). "Activation of the sensory current in salamander olfactory receptor neurons depends on a G protein-mediated cAMP second messenger system." Neuron **6**(5): 825-835.
- Firestein, S., C. Picco, et al. (1993). "The Relation between Stimulus and Response in Olfactory Receptor-Cells of the Tiger Salamander." Journal of Physiology-London **468**: 1-10.
- Firestein, S., G. M. Shepherd, et al. (1990). "Time course of the membrane current underlying sensory transduction in salamander olfactory receptor neurons." Journal of Physiology-London **430**: 135-158.
- Firestein, S. and F. Werblin (1989). "Odor-Induced Membrane Currents in Vertebrate Olfactory Receptor Neurons." Science **244**: 79-82.
- Franco, M. I., L. Turin, et al. (2011). "Molecular vibration-sensing component in *Drosophila melanogaster* olfaction." Proceedings of the National Academy of Sciences of the United States of America **108**(9): 3797-3802.
- Frederickson, C. J. and A. I. Bush (2001). "Synaptically released zinc: Physiological functions and pathological effects." Biometals **14**(3-4): 353-366.
- Frederickson, C. J., L. J. Giblin, et al. (2006). "Concentrations of extracellular free zinc (pZn)(e) in the central nervous system during simple anesthetization, ischemia and reperfusion." Experimental Neurology **198**(2): 285-293.

- Frederickson, C. J., J. Y. Koh, et al. (2005). "The neurobiology of zinc in health and disease." Nature Reviews Neuroscience **6**(6): 449-462.
- Fredholm, B. B., T. Hokfelt, et al. (2007). "G-protein-coupled receptors: an update." Acta Physiologica **190**(1): 3-7.
- Fredrickson, C. J., J.-Y. Koh, et al. (2005). "The neurobiology of zinc in health and disease." Nature Reviews **6**: 449-462.
- Freitag, J., G. Ludwig, et al. (1998). "Olfactory receptors in aquatic and terrestrial vertebrates." Journal of Comparative Physiology A: Neuroethology, Sensory, Neural, and Behavioral Physiology **183**(5): 635-650.
- Frings, S., J. W. Lynch, et al. (1992). "Properties of cyclic-nucleotide gated channels mediating olfactory transduction-activation, selectivity, and blockage properties." Journal of General Physiology **100**(1): 45-67.
- Fulle, H. J., R. Vassar, et al. (1995). "A receptor guanylyl cyclase expressed specifically in olfactory sensory neurons." Proceedings of the National Academy of Sciences of the United States of America **92**(8): 3571-3575.
- Furton, K. G. and L. J. Myers (2001). "The scientific foundation and efficacy of the use of canines as chemical detectors for explosives." Talanta **54**(3): 487-500.
- Gaillard, I., S. Rouquier, et al. (2004). "Olfactory receptors." Cellular and Molecular Life Sciences **61**(4): 456-469.
- Gao, X. L., Z. Y. Du, et al. (2005). "Copper and zinc inhibit G alpha(s) function." Journal of Biological Chemistry **280**(4): 2579-2586.
- Gesteland, R., J. Lettvin, et al. (1965). "Chemical transmission in the nose of the frog." Journal of Physiology-London **181**(3): 525-&.
- Gesteland, R. C. (1964). "Initial events of the olfactogram." Annals of the New York Academy of Sciences **116**: 440-7.
- Getchell, M. L. and T. V. Getchell (1992). "Fine structural aspects of secretion and extrinsic innervation in the olfactory mucosa." Microscopy Research and Technique **23**(2): 111-127.
- Getchell, T. V. (1973). "Analysis of unitary spikes recorded extracellularly from frog olfactory receptor cells and axons." The Journal of physiology **234**(3): 533-551.
- Getchell, T. V. (1986). "Functional Properties of Vertebrate Olfactory Receptor Neurons." Physiology Reviews **66**(3): 772-818.
- Getchell, T. V. and M. L. Getchell (1990). "Regulatory factors in the vertebrate olfactory mucosa." Chemical Senses **15**(2): 223-231.
- Getchell, T. V., F. L. Margolis, et al. (1984). "Perireceptor and receptor events in vertebrate olfaction." Progress in Neurobiology **23**: 317-345.
- Gilad, Y., O. Man, et al. (2005). "A comparison of the human and chimpanzee olfactory receptor gene repertoires." Genome Research **15**(2): 224-230.
- Glusman, G., I. Yanai, et al. (2001). "The complete human olfactory subgenome." Genome Research **11**(5): 685-702.
- Graziadei, G. A. M., F. L. Margolis, et al. (1977). "Immunocytochemistry of olfactory marker protein." Journal of Histochemistry & Cytochemistry **25**(12): 1311-1316.
- Graziadei, P. P. C. and G. A. M. Graziadei (1979). "Neurogenesis and neuron regeneration in the olfactory system of mammals. I. Morphological aspects of differentiation and structural organization of the olfactory sensory neurons." Journal of Neurocytology **8**(1): 1-18.

- Graziadei, P. P. G. (1971). The olfactory mucosa of vertebrates. Chemical senses. L. M. Beidler. Berlin, Springer-Verlag. **4**: 27-58.
- Greer, L. (1991). Structural organization of the olfactory system. Smell and Taste in Health and Disease. T. Getchell, L. M. Bartoshuk and R. Doty. New York, NY, Raven: 65-82.
- Grosmaître, X., L. C. Santarelli, et al. (2007). "Dual functions of mammalian olfactory sensory neurons as odor detectors and mechanical sensors." Nature Neuroscience **10**(3): 348-354.
- Grosmaître, X., A. Vassalli, et al. (2006). "Odorant responses of olfactory sensory neurons expressing the odorant receptor MOR23: A patch clamp analysis in gene-targeted mice." Proceedings of the National Academy of Sciences of the United States of America **103**(6): 1970-1975.
- Gur'ev, D. L., Y. A. Gordopolov, et al. (2006). "Solid-state detonation in the zinc-sulfur system." Applied Physics Letters **88**(2).
- Haffenden, L. J. W., V. A. Yaylayan, et al. (2001). "Investigation of vibrational theory of olfaction with variously labelled benzaldehydes." Food Chemistry **73**(1): 67-72.
- Hamill, O. P., A. Marty, et al. (1981). "Improved patch-clamp techniques for high resolution current recording from cells and cell-free membrane patches." Pflügers Archiv-European Journal of Physiology **391**(2): 85-100.
- Harding, J., P. Graziadei, et al. (1977). "Denervation in the primary olfactory pathway of mice. IV. Biochemical and Morphological Evidence for Neuronal Replacement Following Nerve Section." Brain Research **132**: 11-28.
- Harkema, J. R., S. A. Carey, et al. (2006). "The nose revisited: A brief review of the comparative structure, function, and toxicologic pathology of the nasal epithelium." Toxicologic Pathology **34**(3): 252-269.
- Harper, R. J., J. R. Almirall, et al. (2005). "Identification of dominant odor chemicals emanating from explosives for use in developing optimal training aid combinations and mimics for canine detection." Talanta **67**(2): 313-327.
- Hau, K. M., D. W. Connell, et al. (2000). "Use of partition models in setting health guidelines for volatile organic compounds." Regulatory Toxicology and Pharmacology **31**(1): 22-29.
- Henkin, R. I., B. M. Patten, et al. (1975). "A Syndrome of Acute Zinc Loss." Arch Neurol **32**: 745-751.
- Holbrook, E. H., K. E. M. Szumowski, et al. (1995). "An immunocytochemical, ultrastructural, and developmental characterization of the horizontal basal cells of rat olfactory epithelium." Journal of Comparative Neurology **363**(1): 129-146.
- Horning, M. S. and P. Q. Trombley (2001). "Zinc and copper influence excitability of rat olfactory bulb neurons by multiple mechanisms." Journal of Neurophysiology **86**(4): 1652-1660.
- Hu, J., C. Zhong, et al. (2007). "Detection of near-atmospheric concentrations of CO₂ by an olfactory subsystem in the mouse." Science **317**(5840): 953-957.
- ICAO, I. C. A. O. (1991). Doc. 9571 ICAO Convention, Convention on the marking of plastic explosives for the purpose of identification. U. Nations. Montreal.
- Ishimaru, T., Tsukatani, T., Miwa, T., Furukawa, M. (2000). "Zinc modulates the electro-olfactogram of the frog." Auris Nasus Larynx **27**(3): 257-60.

- Jenkins, T. F., D. C. Leggett, et al. (2001). "Chemical signatures of TNT-filled land mines." Talanta **54**(3): 501-513.
- Johnson, E. W., P. M. Eller, et al. (1993). "An immunoelectron microscopic comparison of olfactory marker protein localization in the supranuclear regions of the rat olfactory epithelium and vomeronasal organ neuroepithelium." Acta Oto-Laryngologica **113**(6): 766-771.
- Johnston, J. (1963). "An application of the steric odor theory." Georgetown Med. Bull **17**: 40.
- Johnston, J. and A. Sandoval (1962). "The stereochemical theory of olfaction. IV. The validity of muskiness as a primary odor." Proc. Sci. Sect. Toilet Goods Assoc. Suppl. **37**: 34.
- Jones, D., R. Augsten, et al. (1995). "Characterization of DMNB, a detection agent for explosives, by thermal analysis and solid state NMR." Journal of Thermal Analysis and Calorimetry **44**(3): 547-561.
- Jones, D. T. and R. R. Reed (1989). "G_{olf}: An Olfactory Neuron Specific-G Protein Involved in Odorant Signal Transduction." Science **244**: 790-795.
- Jones, N. and D. Rog (1998). "Olfaction: a review." The Journal of Laryngology and Otology **112**: 11-24.
- Karlson, P. and M. Luscher (1959). "Pheromones: a New Term for a Class of Biologically Active Substances." Nature **183**(4653): 55-56.
- Kimmelman, C. P. (1993). "Clinical Review of Olfaction." American Journal of Otolaryngology **14**(4): 227-239.
- Kleene, S. J. and R. C. Gesteland (1991). "Calcium-activated Chloride Conductance in Frog Olfactory Cilia." The Journal of Neuroscience **11**(11): 3624-3629.
- Klein, C., T. Heyduk, et al. (2004). "Zinc inhibition of adenylyl cyclase correlates with conformational changes in the enzyme." Cellular Signalling **16**(10): 1177-1185.
- Klein, C., R. K. Sunahara, et al. (2002). "Zinc inhibition of cAMP signaling." Journal of Biological Chemistry **277**(14): 11859-11865.
- Kobilka, B. (1992). "Adrenergic-receptors as models for g-protein-coupled receptors." Annual Review of Neuroscience **15**: 87-114.
- Kobilka, B. K., T. S. Kobilka, et al. (1988). "Chimeric alpha-2-adrenergic, beta-2-adrenergic receptors- delineation of domains involved in effector coupling and ligand-binding specificity." Science **240**(4857): 1310-1316.
- Kruse, A. (2007). "Defense Sciences Research and Technology Special Focus Area: RealNose <http://www.darpa.mil/dso/solicitations/baa07-21mod11.htm>."
- Kruyt, H. R. (1952). Colloid Science. New York, Elsevier.
- Kurahashi, T. (1989). "Activation by Odorants of Cation-Selective Conductance in the Olfactory Receptor Cell Isolated from the Newt." Journal of Physiology-London **419**: 177-192.
- Lancet, D., N. Benarie, et al. (1994). "Mapping the Superfamily of G-Protein Coupled Receptors in Olfaction." Journal of Neurochemistry **63**: S2-S2.
- Laska, M., D. Joshi, et al. (2006). "Olfactory sensitivity for aliphatic aldehydes in CD-1 mice." Behavioural Brain Research **167**(2): 349-354.
- Ma, M. H. (2007). "Encoding olfactory signals via multiple chemosensory systems." Critical Reviews in Biochemistry and Molecular Biology **42**(6): 463-480.

- Ma, M. H., W. R. Chen, et al. (1999). "Electrophysiological characterization of rat and mouse olfactory receptor neurons from an intact epithelial preparation." Journal of Neuroscience Methods **92**(1-2): 31-40.
- Mackay-Sim, A. and I. E. Dreosti (1989). "Olfactory Function in zinc-deficient adult mice." Exp Brain Res **76**: 207-212.
- Malnic, B., J. Hirono, et al. (1999). "Combinational Receptor Codes for Odors." Cell **96**: 713-723.
- McBride, K., B. Slotnick, et al. (2003). "Does intranasal application of zinc sulfate produce anosmia in the mouse? An olfactometric and anatomical study." Chemical Senses **28**(8): 659-670.
- Menco, B. P. M. (1997). "Ultrastructural Aspects of Olfactory Signaling." Chemical Senses **22**: 295-311.
- Menco, B. P. M., R. C. Bruch, et al. (1992). "Ultrastructural localization of olfactory transduction components: the G protein subunit Golf[alpha] and type III adenylyl cyclase." Neuron **8**(3): 441-453.
- Menco, B. P. M. and J. E. Jackson (1997). "A banded topography in the developing rat's olfactory epithelial surface." Journal of Comparative Neurology **388**(2): 293-306.
- Menco, B. P. M. and E. E. Morrison (2003). Morphology of the Mammalian Olfactory Epithelium: Form, Fine Structure, Function, and Pathology. Handbook of Olfaction and Gustation. R. L. Doty. New York, Marcel Dekker, Inc.,: 17-49.
- Meyer, M. R., A. Angele, et al. (2000). "A cGMP-signaling pathway in a subset of olfactory sensory neurons." Proceedings of the National Academy of Sciences of the United States of America **97**(19): 10595-10600.
- Minic, J., M.-A. Persuy, et al. (2005). "Functional expression of olfactory receptors in yeast and development of a bioassay for odorant screening." FEBS Journal **272**(2): 524-537.
- Mombaerts, P. (1999). "Molecular biology of odorant receptors in vertebrates." Annual Review of Neuroscience **22**: 487-509.
- Moncrieff, R. (1949). "A new theory of odour." Perfumery & Essential Oil Record **40**: 279-285.
- Moran, D. T., J. C. Rowley, et al. (1982). "The fine-structure of the olfactory mucosa in man." Journal of Neurocytology **11**(5): 721-746.
- Morrison, E. E. (1995). Anatomy and Ultrastructure of the Human Olfactory Neuroepithelium Handbook of Olfaction and Gustation. R. Doty. New York, Marcel Dekker, Inc.
- Morrison, E. E. and R. M. Costanzo (1990). "Morphology of the Human Olfactory Epithelium." The journal of comparative neurology **297**: 1-13.
- Morrison, E. E. and R. M. Costanzo (1992). "Morphology of olfactory epithelium in humans and other vertebrates." Microscopy Research and Technique **23**(1): 49-61.
- Morrison, E. E. and D. T. Moran (1995). Anatomy and Ultrastructure of the Human Olfactory Neuroepithelium Handbook of Olfaction and Gustation. R. Doty. New York, Marcel Dekker, Inc.
- Munger, S. D., T. Leinders-Zufall, et al. (2009). "Subsystem Organization of the Mammalian Sense of Smell." Annual Review of Physiology **71**: 115-140.
- Myers, L. (2008). Canine LOD for eugenol measured by olfactometer, gas-spectrometer and double mass-spectrophotometer. . Auburn.

- Nakashima, M., K. Mori, et al. (1978). "Centrifugal influence on olfactory bulb activity in the rabbit." Brain research **154**(2): 301-316.
- Nespoulous, C., L. Briand, et al. (2004). "Odorant Binding and Conformational Changes of a Rat Odorant-binding Protein." Chemical Senses **29**(3): 189-198.
- Ngai, J., M. M. Dowling, et al. (1993). "The family of genes encoding odorant receptors in the channel catfish." Cell **72**(5): 657-666.
- Nickell, W. T., N. K. Kleene, et al. (2007). "Mechanisms of neuronal chloride accumulation in intact mouse olfactory epithelium." J Physiol **583**(3): 1005-1020.
- Nomura, T., S. Takahashi, et al. (2004). "Cytoarchitecture of the normal rat olfactory epithelium: Light and scanning electron microscopic studies." Archives of Histology and Cytology **67**(2): 159-170.
- Odowd, B. F., M. Hnatowich, et al. (1989). "Palmitoylation of the human beta-2-adrenergic receptor - mutation of cys-341 in the carboxyl tail leads to an uncoupled nonpalmitoylated form of the receptor." Journal of Biological Chemistry **264**(13): 7564-7569.
- Olender, T., T. Fuchs, et al. (2004). "The canine olfactory subgenome." Genomics **83**(3): 361-372.
- Ottoson, D. (1956). "Analysis of the electrical activity of the olfactory epithelium." Acta Physiologica Scandinavica **35**: 7-83.
- Ottoson, D. (1960). "Studies on Slow Potentials in the Rabbit's Olfactory Bulb and Nasal Mucosa." Acta Physiologica Scandinavica **47**(2-3): 136-148.
- Ottoson, D. (1971). The Electro-Olfactogram: A Review of Studies on the Receptor Potential of the Olfactory Organ. Handbook of sensory physiology. Beidler LM. Berlin., Springer. **4**: 95-131.
- Pace, U., E. Hanski, et al. (1985). "Odorant-sensitive adenylate cyclase may mediate olfactory reception." Nature **316**: 255-258.
- Pelosi, P. (1994). "Odorant-Binding Proteins." Critical Reviews in Biochemistry and Molecular Biology **29**(3): 199-228.
- Pevsner, J., P. B. Sklar, et al. (1986). "Odorant-binding protein: localization to nasal glands and secretions." Proceedings of the National Academy of Sciences of the United States of America **83**(13): 4942-6.
- Pevsner, J. and S. H. Synder (1990). "Odorant binding protein: odorant transport function in the vertebrate nasal epithelium." Chemical Senses **15**(2): 217-222.
- Phillips, J. O. and A. F. Fuchs, Eds. (1989). Gustation and Olfaction. Textbook of Physiology: Excitable Cells and Neurophysiology. Philadelphia, W.B. Saunders Company.
- Pinato, G., J. Rievaj, et al. (2008). "Electroolfactogram responses from organotypic cultures of the olfactory epithelium from postnatal mice." Chemical Senses **33**(4): 397-404.
- Preziuso, L. (1927). "La superficie de la mucosa olfativa en los mamíferos domestica." Nuovo Ecol. **32**: 113-126, 135-139.
- Quignon, P., M. Giraud, et al. (2005). "The dog and rat olfactory receptor repertoires." Genome Biology **6**(10): 9.
- Quignon, P., E. Kirkness, et al. (2003). "Comparison of the canine and human olfactory receptor gene repertoires." Genome Biology **4**(12): 9.

- Rafols, J. A. and T. V. Getchell (1983). "Morphological Relations Between the Receptor Neurons, Sustentacular Cells and Schwann Cells in the Olfactory Mucosa of the Salamander." The Anatomical Record **206**: 87-101.
- Reed, R. R. (1992). "Signaling Pathways in Odorant Detection." Neuron **8**: 205-209.
- Ressler, K. J., S. L. Sullivan, et al. (1993). "A Zonal Organization of Odorant Receptor Gene Expression in the Olfactory Epithelium." Cell **73**: 597-609.
- Restrepo, D., Teeter John H., and Detlev Schild (1996). "Second Messenger Signaling in Olfactory Transduction." Journal of Neurobiology **30**(1): 37-48.
- Samoylov, A. M., T. I. Samoylova, et al. (2005). "Novel Metal Clusters Isolated from Blood Are Lethal to Cancer Cells." Cells Tissues Organs **179**: 155-124.
- Sandhya, K. and M. C. Vemuri (1997). "Regulation of cellular signals by G-proteins." Journal of Biosciences **22**(3): 375-397.
- Satir, P. and S. T. Christensen (2007). "Overview of structure and function of mammalian cilia." Annual Review of Physiology **69**: 377-400.
- Saunders, H. (1962). "The stereochemical theory of olfaction. V. Some odor observation in terms of the Amoore theory." Proc. Sci. Sect. Toilet Goods Assoc. Suppl. **37**: 46.
- Schandar, M., K. L. Laugwitz, et al. (1998). "Odorants selectively activate distinct G protein subtypes in olfactory cilia." Journal of Biological Chemistry **273**(27): 16669-16677.
- Scott, J. W. and P. E. Scott-Johnson (2002). "The Electroolfactogram: A Review of Its History and Uses." Microscopy Research and Technique **58**: 152-160.
- Seebungkert, B. and J. W. Lynch (2002). "Effects of polyunsaturated fatty acids on voltage-gated K⁺ and Na⁺ channels in rat olfactory receptor neurons." European Journal of Neuroscience **16**(11): 2085-2094.
- Seifert, K. (1971). "Licht- und elektronenmikroskopische untersuchungen der Bowman-Drüsen in der riechschleimhaut makrosomatischer säuger." European Archives of Oto-Rhino-Laryngology **200**(3): 252-274.
- Shepherd, G., T. Getchell, et al. (1975). Analysis of structure and function in the olfactory pathway. New York, NY, Raven.
- Shepherd, G. M. (1994). "Discrimination of Molecular Signals by the Olfactory Receptor Neuron." Neuron **13**(4): 771-790.
- Sinnarajah, S., C. W. Dessauer, et al. (2001). "RGS2 regulates signal transduction in olfactory neurons by attenuating activation of adenylyl cyclase III." Nature (London, United Kingdom) **409**(6823): 1051-1055.
- Sinnarajah, S., P. I. Ezeh, et al. (1998). "Inhibition and enhancement of odorant-induced cAMP accumulation in rat olfactory cilia by antibodies directed against Gas/olf- and Gai-protein subunits." FEBS Letters **426**(3): 377-380.
- Slotnick, B. (2006). "Olfactory epithelium and olfaction in zinc-treated mice." Chemical Senses **31**(8): 326.
- Slotnick, B., P. Glover, et al. (2000). "Does intranasal application of zinc sulfate produce anosmia in the rat?" Behavioral Neuroscience **114**(4): 814-829.
- Slotnick, B., A. Sanguino, et al. (2007). "Olfaction and olfactory epithelium in mice treated with zinc gluconate." Laryngoscope **117**(4): 743-749.
- Spehr, M. and S. D. Munger (2009). "Olfactory receptors: G protein-coupled receptors and beyond." Journal of Neurochemistry **109**(6): 1570-1583.

- Steinfeld, J. I. and J. Wormhoudt (1998). "Explosives detection: A challenge for physical chemistry." Annual Review of Physical Chemistry **49**: 203-232.
- Strotmann, J., I. Wanner, et al. (1994). "Rostr-caudal patterning of receptor-expressing olfactory neurones in the rat nasal cavity." Cell Tissue Res. **278**: 11-20.
- Strotmann, J., I. Wanner, et al. (1994). "Olfactory neurones expressing distinct odorant receptor subtypes are spatially segregated in the nasal neuroepithelium." Cell Tissue Res. **276**: 429-438.
- SWGDOG (2007) "substance detector dogs, explosives detection."
<http://alean.com/documents/swgdog.pdf>.
- Takeda, A., M. Ohnuma, et al. (1997). "Zinc transport in the rat olfactory system." Neuroscience Letters Volume 225: 69-71.
- Takeuchi, H. and T. Kurahashi (2005). "Mechanism of signal amplification in the olfactory sensory cilia." Journal of Neuroscience **25**(48): 11084-11091.
- Thomas, J. M. (1988). "Colloidal Metals - Past, Present and Future." Pure and Applied Chemistry **60**(10): 1517-1528.
- Turin, L. (1996). "A Spectroscopic Mechanism for Primary Olfactory Reception." Chem. Senses **21**: 773-791.
- Ueki, S. and E. F. Domino (1961). "Some evidence for a mechanical receptor in olfactory function." Journal of Neurophysiology **24**(1): 12-&.
- Vassar, R., J. Ngai, et al. (1993). "Spatial Segregation of Odorant Receptor Expression in the Mammalian Olfactory Epithelium." Cell **74**: 309-318.
- Viswaprakash, N., J. C. Dennis, et al. (2009). "Enhancement of Odorant-Induced Response in Olfactory Receptor Neurons by Zinc Nanoparticles." Chem. Senses **34**: 547-557.
- Viswaprakash, N., E. M. Josephson, et al. (2010). "Odorant Response Kinetics from Cultured Mouse Olfactory Epithelium at Different Ages in vitro." Cells Tissues Organs **192**(6): 361-373.
- Vodyanoy, V. (2010). "Zinc nanoparticles interact with olfactory receptor neurons." Biometals **23**(6): 1097-1103.
- Wright, N. T., J. W. Margolis, et al. (2005). "Refinement of the solution structure of rat Olfactory Marker Protein (OMP)." Journal of Biomolecular Nmr **33**(1): 63-68.
- Wynn, C. M., S. Palmacci, et al. (2010). "Noncontact detection of homemade explosive constituents via photodissociation followed by laser-induced fluorescence." Optics Express **18**(6): 5399-5406.
- Yinon, J. (2003). "Detection of explosives by electronic noses." Analytical Chemistry **75**(5): 99A-105A.
- Yinon, J. (2005). "Detection of hidden explosives: Techniques and applications - an overview." Abstracts of Papers of the American Chemical Society **230**: U327-U327.
- Yinon, J. (2006). "Detection of hidden explosives: An overview." American Laboratory **38**(12): 18-+.
- Zhang, X. M. and S. Firestein (2002). "The olfactory receptor gene superfamily of the mouse." Nature Neuroscience **5**(2): 124-133.
- Zhou, Y., A. J. Illies, et al. (1993). "Concentration of odorant compounds through interaction with the biological receptor lysine." Langmuir **9**(6): 1483-5.

- Zufall, F., S. Firestein, et al. (1991). "Analysis of single cyclic nucleotide-gated channels in olfactory receptor cells " Journal of Neuroscience **11**(11): 3573-3580.
- Zufall, F., H. Hatt, et al. (1993). "Rapid application and removal of second messengers to cyclic nucleotide-gated channels from olfactory epithelium." Proc. Natl. Acad. Sci. USA **90**: 9335-9339.